High-resolution Inference of Multiplexed Anti-HIV Gene Editing using Single-Cell Targeted DNA Sequencing

Mohamed S. Bouzidi[1,2], Zain Y. Dossani[1,2], Carolina Di Benedetto[3], Kyle A. Raymond[1,4], Shivani Desai[1], Leonard R. Chavez[1,5], Paola Betancur[3], Satish K. Pillai[1,2,*]

[1]Vitalant Research Institute, San Francisco, CA, USA.
[2]Department of Laboratory Medicine, University of California, San Francisco, CA, USA.
[3]Department of Radiation Oncology, University of California, San Francisco, CA, USA.
[4]Department of Virology, Institut Pasteur, Université de Paris, CNRS UMR3569, Paris, France.
[5]Rewrite Therapeutics, Berkeley, CA, USA.

*Correspondence should be addressed to: Satish K. Pillai, Ph.D.

Email: satish.pillai@ucsf.edu

Short title: Single-Cell Analysis of Anti-HIV Gene Editing

Competing Interest Statement: No competing interests.

Keywords: HIV, CRISPR/Cas9, single-cell sequencing, antiviral gene editing, myeloid cells

This PDF file includes:

Main Text
Figures 1 to 6
Supplementary Figures 1 to 2
Supplementary Table 1

Abstract

Gene therapy-based HIV cure strategies typically aim to excise the HIV provirus directly, or target host dependency factors (HDFs) that support viral persistence. Cure approaches will likely require simultaneous co-targeting of multiple sites within the HIV genome to prevent evolution of resistance, and/or co-targeting of multiple HDFs to fully render host cells refractory to HIV infection. Bulk cell-based methods do not enable inference of co-editing within individual viral or target cell genomes, and do not discriminate between monoallelic and biallelic gene disruption. Here, we describe a targeted single-cell DNA sequencing (scDNA-seq) platform characterizing the near full-length HIV genome and 50 established HDF genes, designed to evaluate anti-HIV gene therapy strategies. We implemented the platform to investigate the capacity of multiplexed CRISPR-Cas9 ribonucleoprotein complexes (Cas9-RNPs) to simultaneously 1) inactivate the HIV provirus, and 2) knockout the *CCR5* and *CXCR4* HDF (entry co-receptor) genes in microglia and primary monocyte-derived macrophages (MDMs). Our scDNA-seq pipeline revealed that antiviral gene editing is rarely observed at multiple loci (or both alleles of a locus) within an individual cell, and editing probabilities across sites are linked. Our results demonstrate that single-cell sequencing is critical to evaluate the true efficacy and therapeutic potential of HIV gene therapy.

43 **eTOC Synopsis**

44

45 Bouzidi et al created a novel targeted single-cell DNA sequencing pipeline to characterize anti-
46 HIV gene editing at multiple viral and host genome sites within individual cells, providing the HIV
47 cure field with a powerful tool to gauge the preclinical and clinical efficacy of HIV gene therapy
48 approaches.

49

Introduction

Despite the advent of antiretroviral therapy (ART), the human immunodeficiency virus (HIV) was responsible for the deaths of 650,000 people worldwide in 2021, while 38.4 million individuals are currently living with HIV infection.[1] Moreover, ART needs to be taken on a lifelong basis due to the persistence of HIV latently-infected cells during treatment, which typically reinitiate spreading infection when ART is stopped.[2,3] As access to lifelong ART is extremely challenging in resource-limited settings where HIV predominates, there is a desperate need for effective prophylactic and curative strategies.[4,5]

Several HIV cure strategies are currently in development, including “shock-and-kill”,[6] “block-and-lock”[7], and oncology-derived immunomodulatory[8] and bone marrow transplantation approaches targeting the latent HIV reservoir.[9–11] The discovery of the CRISPR (Clustered Regularly Interspaced Short Palindromic Repeats)-Cas9 gene editing system has raised new hopes for gene therapy-based HIV cure strategies.[12–14] The Cas9 enzyme interacts with the scaffold sequence of a guide RNA (gRNA) complementary to a target sequence, enabling knockout of a targeted gene in a highly specific manner.[15] HIV gene therapy-based cure strategies in development typically aim to excise the HIV provirus directly,[16–22] or target host dependency factors (HDFs) including viral entry receptors that support viral persistence.[23–25] In recent years, a number of preclinical HIV cure studies have showed promising results using this technology.[26–31] An important caveat, however, arises from the high mutation and recombination rate of HIV-1,[32,33] which allows the virus to navigate broad expanses of sequence space in short periods of time. Studies of CRISPR-based HIV excision strategies targeting the viral genome at a single site demonstrate rapid evolution of viral resistance to the gene editing modality, mirroring the evolution of antiviral drug resistance in the setting of monotherapy.[34–38] Therefore, the HIV genome will

need to be targeted at multiple sites simultaneously. Drawing from lessons learned during the development of combination ART, a minimum of three distinct genome sites may need to be targeted to prevent evolution of resistance.[16] Similarly, the neutralization of a single HDF supporting HIV replication is unlikely to completely protect cells from infection, suggesting that multiple HDFs will likely need to be targeted simultaneously to achieve a functional or sterilizing cure for HIV infection.[16] Even when considering a single HDF locus, genes exhibiting codominance between alleles will likely require biallelic knockout to fully eliminate generation of the encoded protein and, in this manner, block viral infection. Illustration of this concept is provided in nature; CCR5-Δ32 heterozygotes typically produce enough CCR5 protein at the target cell surface to support HIV replication, while Δ32 homozygotes are fully protected from HIV infection (by the highly prevalent CCR5-tropic HIV strains).[39–41]

Based on the need for multitargeting to achieve an HIV cure, molecular diagnostics enabling detection of multiple edits within individual cells will be critical in assessing the true, real-world potency of anti-HIV gene therapy approaches. Currently-implemented technologies, including Sanger sequencing of bulk cell populations and gel-based imaging of excision products, do not enable inference of co-editing within single cells.[42] Furthermore, standard deep sequencing approaches will not suffice, due to read length limitations that prevent inference of genetic linkage between distal sites.[42] To address this need, we report here a novel, targeted single-cell DNA sequencing (scDNA-seq) pipeline featuring a hybrid experimental and computational structure to characterize anti-HIV gene editing at viral and host genome sites with extreme resolution. Our platform characterizes the near full-length HIV genome and 50 established HDF genes (identified in a primary cell-based CRISPR screen) at the single-cell level. We implemented the platform to investigate the capacity of multiplexed CRISPR-Cas9 ribonucleoprotein complexes (Cas9-RNPs) to simultaneously 1) inactivate the HIV provirus, and

100 2) knockout the *CCR5* and *CXCR4* HDF (entry co-receptor) genes in microglia and primary
101 monocyte-derived macrophages (MDMs). Our findings demonstrate the utility and critical
102 importance of scDNA-seq analysis to accurately and comprehensively evaluate the efficacy of
103 antiviral gene editing strategies.
104
105 **Results**
106
107 **Generation and validation of a customized panel allowing detection of CRISPR-Cas9**
108 **edits in the near-full length HIV provirus and HIV HDFs at the single-cell level**
109 To develop our single-cell sequencing strategy to detect CRISPR-Cas9 editing, we first designed
110 a sequencing primer panel. To evaluate gene editing within both the HIV provirus and HDFs
111 supporting viral replication, we designed a panel targeting tiled amplicons spanning the HIV
112 genome, and 53 HDF genes that were previously identified using a genome-wide CRISPR screen
113 in primary CD4+ T cells (e.g. *CXCR4*, *CCR5* and *CD4*, which also facilitate HIV entry into myeloid
114 cells).[43] All targeted genes, chromosomal positions, primer pair names, sequences, and genome
115 coordinates are described in the supplementary materials (Supp. Table 1). Thirty-six primer pairs
116 cover the HIV genome from position 30 to position 9516 based on the HIV HXB2 reference
117 genome (Figure 1). This includes the 5' long terminal repeat (LTR) region, which has been
118 targeted specifically in several HIV gene therapy strategies,[16,26–30,44] allowing detection of edits in
119 highly conserved regions such as the Primer Binding Site (PBS) and packaging signals (PSI
120 sequences).
121
122 **Bulk cell and single-cell sequencing analyses provide concordant estimates of antiviral**
123 **gene editing efficiencies.**

124 In order to test our single-cell sequencing approach, we first targeted the HIV 5'LTR along with
125 the host HIV co-receptor genes *CXCR4* and *CCR5* using CRISPR-Cas9 RNP complexes. We
126 first tested our approach in the HC69.5 cell line, a clone derived from the C20 immortalized
127 microglial cell that has been infected with an HIV-derived construct.[45] The presence of a d2eGFP
128 sequence under the control of the viral promoter permits the detection of viral expression through
129 flow cytometry measurement of GFP signal. We nucleofected HC69.5 cells with RNPs targeting
130 the HIV 5'LTR, *CXCR4* and *CCR5* and evaluated editing efficiency using our scDNA-seq platform,
131 Sanger sequencing and TIDE analysis, and flow cytometry (Figure 2A).
132
133 In regards to coverage across the HIV genome (Supplementary Figure 1A), we observed a gap
134 in coverage between amplicons 6 and amplicon 21. This reflects the fact that the provirus in the
135 HC69.5 clone lacks the corresponding region of the HIV genome (consisting of a part of *gag* and
136 the whole *pol* gene). We independently evaluated and validated the performance of our panel by
137 applying our scDNA-seq pipeline to the J-Lat cell line (Jurkat cells harboring a near-complete,
138 latent HIV proviral genome). The read depths observed across amplicons indicate robust
139 coverage across the HIV provirus (Supplementary Figure 1B). Similar metrics were generated for
140 the host genes indicating robust coverage (Supplementary Figure 1B and C).
141
142 We next evaluated gene editing efficiencies at viral and host loci using both Sanger (bulk) and
143 single-cell NGS approaches. Three measurements were generated for each targeted site: 1)
144 TIDE analysis of Sanger bulk sequencing data, 2) Pseudo-bulk analysis of single-cell NGS data
145 using CRISPResso2 software (ignoring single-cell barcodes), and true single-cell analysis using
146 CRISPResso2 (interpreting single-cell barcodes). Overall, the three distinct analytical methods
147 (leveraging two distinct sequencing approaches) provided highly concordant estimates of gene
148 editing efficiencies at all three loci (Figure 3). We observed high editing efficiencies in the HIV

149 LTR and *CXCR4* (mean efficiency of 74.75 and 60.7%, respectively), while editing of *CCR5* as
150 measured by all three methods was less efficient (21.11% mean editing efficiency) (Figure 3A).
151
152 The observed highly potent editing of the HIV LTR was correlated with a 90% reduction of GFP
153 signal in edited cells as compared to cells nucleofected with control guides (44.8% to 4.82%)
154 (Figure 3C), demonstrating the accuracy of our sequence-based inference of gene editing.
155
156 In addition to immortalized microglia, we applied our scDNA-seq pipeline to infer antiviral gene
157 editing in primary monocyte-derived macrophages (MDMs), which are key constituents of the
158 latent HIV reservoir *in vivo* that will likely need to be targeted by HIV cure strategies.[46] We isolated
159 monocytes from freshly-collected blood, and nucleofected them with *CXCR4*- and *CCR5*-
160 targeting RNPs. After a 7-day M-CSF treatment, MDMs were harvested and characterized by
161 genetic and immunophenotypic analyses (Figure 2B). As it is known that CRISPR editing can
162 impact cell function and metabolism, we first sought to evaluate the impact of editing on
163 macrophage immune function. We incubated edited and unedited cells with fluorescent beads
164 and measured phagocytic uptake by macrophages using flow cytometry (Supplementary Figure
165 2). We observed a similar level of phagocytosis in edited and unedited cells, demonstrating that
166 a key macrophage immune function was not impacted by nucleofection or Cas9 activity.
167
168 Similar to our observations in immortalized microglia, bulk-cell and single-cell analyses provided
169 highly concordant estimates of gene editing efficiencies in primary MDMs. We observed high
170 editing efficiency in *CXCR4* (mean efficiency of 73.52%), while editing of *CCR5* as measured by
171 all three methods was once again less efficient (17.54% mean editing efficiency) (Figure 3B).
172

173 **Single-cell sequencing enables highly-precise characterization of CRISPR-induced indel**
174 **spectra.**
175 Precisely characterizing the indel spectra induced by CRISPR gene editing is critical to evaluating
176 therapeutic efficacy and safety. It is now known that the CRISPR-induced indel spectrum is
177 correlated with editing efficiency at a specific site; the less diverse the indel spectrum, the higher
178 the editing efficiency.[47] We therefore sought to determine if our scDNA-seq pipeline enabled
179 higher-resolution characterization of indel spectra as compared to standard Sanger sequencing
180 and TIDE analysis. Our analyses unequivocally demonstrate that scDNA-seq identifies CRISPR-
181 induced indel spectra with significantly enhanced sensitivity ($p=0.025$, paired t test), typically
182 revealing a broad range of indels and minority variants (Figure 4). In contrast, Sanger sequencing
183 only enables detection of dominant, majority indel variants (Figure 4).
184
185 **Single-cell sequencing enables inference of antiviral gene editing at multiple loci within**
186 **individual cells**
187 HIV enters target cells such as T cells and myeloid cells using the CD4 receptor and the CXCR4
188 or CCR5 co-receptors. It has been described that a switch occurs during the course of HIV
189 infection, in favor of one or the other co-receptor.[48] It is therefore necessary to knock-out both co-
190 receptors to avoid a switch, preventing viral rebound. Leveraging our single cell sequencing
191 approach, we sought to evaluate co-editing efficiency at a single-cell level in HC69.5 and primary
192 MDMs. We processed our single-cell sequencing data through CRISPRessoV2 software (as
193 described in the Materials and Methods), and summarized the data in Figure 5. Each line
194 represents one cell, characterized by its editing frequency at each targeted site. The shade of
195 green indicates the editing frequency (dark green for high editing frequency to white for low editing
196 frequency) (Figure 5A&B) Full co-editing (editing of all targets) was observed in 37.4% of HC69.5
197 cells (Figure 5C) and in 22.38% of primary macrophages (Figure 5D). The single-cell resolution

198 of our analysis demonstrates the extreme heterogeneity of antiviral gene editing patterns across
199 cells (Figure 5), informing therapeutic efficacy while demonstrating that cell-specific factors likely
200 modulate the intake and activity of gene editing machinery.
201

202 **Single-cell sequencing enables allele-specific evaluation of antiviral gene editing**
203 **performance**

204 This single-cell approach also allows us to survey editing in each of the two alleles of each
205 targeted host gene.[49] This is of particular importance as editing on one chromosome may not be
206 enough to fully shut down the expression of a HDF and prevent HIV infection. For this purpose,
207 we categorized allele-specific editing based on observed editing efficiencies (defined as the
208 frequency of NGS reads harboring indels); genes with an editing efficiency above 0.8 were
209 considered to be edited at both alleles, genes with an editing efficiency value between 0.2 and
210 0.8 were considered to be edited at only one allele, and genes with an editing efficiency below
211 0.2 were categorized as non-edited (Figure 5A&B). We observed that 43% of the HC69.5 cells
212 were $CXCR4^{mut}/CXCR4^{mut}$ and 42% $CXCR4^{wt}/CXC4^{mut}$. For CCR5, we observed that 10% of the
213 cells $CCR5^{mut}$ /$CCR5^{mut}$ and 36% of the cells were $CCR5^{wt}/CCR5^{mut}$ (Figure 5C). In primary
214 macrophages, approximately 57% $CXCR4^{mut}/CXCR4^{mut}$ and 28% of the cells were
215 $CXCR4^{wt}/CXCR4^{mut}$. For *CCR5*, we observed that 4% $CCR5^{mut}/CCR5^{mut}$ and 21% of cells were
216 $CCR5^{wt}/CCR5^{mut}$ (Figure 5D). This result may partially explain the moderate decrease of CCR5
217 expression in edited MDMs, as only 4% of the cells exhibited biallelic disruption of the CCR5 HDF
218 gene.
219

220 **Gene editing events exhibit interdependence**

221 Finally, we leveraged the power of our single-cell inference approach to determine whether
222 antiviral gene editing events occur independently of one another. We built contingency tables for

223 each gene pair across both tested cell types (*HIV-LTR*, *CXCR4* and *CCR5* for HC69.5 and
224 *CXCR4* and *CCR5* for MDMs) and determined if the co-occurrence of editing at both considered
225 sites was observed more or less than expected (assuming that there are independent probabilities
226 of editing at each targeted site). We observed that in both HC69.5 and MDMs, mono-editing
227 (editing at a single targeted locus) was lower compared to the expected value, while co-editing
228 and co editing frequency was higher than expected (Figure 6A, Fisher's exact t-test p-values
229 ranging from 0.003 to <0.0001). Similarly, we sought to determine if editing at two alleles could
230 be explained by independent probabilities. Again, we obsesrved higher than expected frequencies
231 of co-editing, suggesting that antiviral gene editing events are not independent (Figure 6B&C) ,
232 p-value ≤ 0.001).
233
234 **Discussion**
235
236 Anti-HIV gene therapy will likely require editing of multiple host genes and/or sites in the proviral
237 genome. According to mathematical models, more than 99% of total provirus in people living with
238 HIV needs to be inactivated to achieve a functional cure.[16] Provirus inactivation requires editing
239 on several sites due to viral genetic diversity and plasticity, which may result in the generation of
240 escape mutants considering the exceptional adaptability of HIV.[37] Moreover, it is unlikely that 99%
241 of infected cells will be targeted by the CRISPR-Cas9 system: some macrophages for example
242 can infiltrate deep into tissues, where delivery of the CRISPR payload can be very challenging.
243 One way to overcome this issue is to target HDFs such as HIV co-receptors *CXCR4* and *CCR5*
244 to prevent viral spread from cells harboring unedited provirus. In this case, mathematical models
245 predict that inactivating provirus in 60% of the infected cells and reducing the pool of susceptible
246 cells by 68% is enough to achieve a functional cure.[16]

247 So far, no method has been proposed to rigorously assess the frequencies of such events *in vitro*
248 or *in vivo*. Here, we demonstrate that single-cell encapsulation and targeted next generation
249 sequencing, in combination with a specific bioinformatic pipeline, is a reliable and powerful
250 method to characterize antiviral gene editing in both cell lines and primary cells. The editing
251 efficiencies measured with our single-cell method are close but not identical to the results
252 obtained with Sanger sequencing and TIDE analysis. The difference observed between the two
253 methods can likely be explained by the reduced sensitivity of Sanger sequencing in comparison
254 to NGS approaches,[50] resulting in minority genetic variants being excluded from the final results.
255
256 Highly precise CRISPR editing at a targeted site is key to avoid lethal editing or production of
257 aberrant cells. It has been shown that indel spectra directly correlate with editing precision and
258 efficiency; the less diverse the indels, the more precise and potent the editing. However, Sanger
259 sequencing and TIDE analysis do not capture indel spectra with sufficient sensitivity, as revealed
260 by our analyses. We demonstrated that indel spectra characterized with our single-cell approach
261 were significantly more detailed and reliable than spectra obtained through TIDE, revealing
262 several indel variants that were unseen in population sequencing data. This result is of particular
263 importance when evaluating a therapeutic approach to predict gene editing efficiency and overall
264 editing precision.
265
266 Single-cell sequencing is the only method that enables inference of co-editing events within the
267 same targeted cell. Our results demonstrate that the frequency of co-editing events cannot simply
268 be predicted by considering the product of editing efficiencies across individual loci due to linkage
269 effects. Single cell sequencing also allows us to determine if gene editing is bi-allelic or mono-
270 allelic; this is critical as neutralization of both alleles is often required to completely abrogate target
271 protein expression. In this study, we were able to achieve 42% mono-allelic editing and 43% bi

272 allelic-editing on the *CXCR4* gene in HC69.5 cells. For the *CCR5* gene, 36% of the cells showed
273 mono-allelic editing and 10% bi-allelic editing. The results for *CCR5* reveal a considerable bias
274 towards mono-allelic editing for this locus. Similar results were observed for primary MDMs, where
275 bi-allelic editing of *CXCR4* was observed in 57% versus 28% for mono-allelic editing. For *CCR5*,
276 21% of the cells were edited in one allele and 3.5% of the cells in both alleles. Interestingly, flow
277 cytometry data for the latter case showed a decrease of 11.3% in the frequency of CCR5-
278 expressing cells compared to the control, and a 13% decrease in mean fluorescence intensity
279 (MFI) (data not shown), without any impact on cell function (as represented by phagocytic
280 activity). This demonstrates that the relationship between gene editing and protein expression is
281 complex, and in some cases, the intact allele may compensate for the knockout allele resulting in
282 a lower-than-expected impact on protein expression. These results highlight the need for a
283 comprehensive method to evaluate gene editing activity such as the single cell approach used
284 here.
285
286 The fact that our observed gene editing frequencies across loci and alleles on a cellular level
287 were not independent suggests that some cells may be more permissive than others to editing.
288 The permissiveness of a cell to Cas9-RNPs could be due to several factors: the efficiency of
289 nuclear transport machinery, epigenetic factors such as chromatin state or methylation, or DNA
290 repair machinery.
291
292 In conclusion, our study demonstrates that our single-cell pipeline is a powerful approach to
293 evaluate the potency of multi-targeting antiviral gene editing strategies. It yields critical insights
294 into co-editing events across targeted loci and alleles, of key relevance to anti-HIV gene therapy.
295 Our method and panel design can be further expanded to survey a broad range of
296 bioinformatically-predicted off-target sites, to determine the specificity and safety of gene therapy

297 approaches. In addition, our panel can be expanded to reliably characterize non-subtype B
298 proviruses, which will be an essential developmental step when evaluating therapeutic efficacy in
299 diverse global settings. In combination with rational guide design and continuing innovation in the
300 engineering of gene editing machinery, our single-cell sequencing approach provides another key
301 tool to facilitate the clinical development of cure-focused HIV gene therapy approaches.
302
303 **Materials and Methods**
304
305 *Primary Human Monocyte Isolation*
306 Primary monocytes were isolated from blood obtained from healthy donors (Vitalant, San
307 Francisco, CA). A total of 15 mL of blood from TRIMA residual was diluted at a 1:1 ratio with a
308 3mM EDTA PBS 2% FBS buffer. The resulting mixture was layered onto a Ficoll-Paque density
309 gradient medium and centrifuged at 1200 g for 30 minutes at room temperature. The peripheral
310 blood mononuclear cell (PBMC) layer was carefully collected and subsequently resuspended in
311 500 µL of ACK lysis buffer (Gibco), followed by a 3-minute incubation at room temperature. To
312 this, 40 mL of 3mM EDTA PBS 2% FBS buffer was added, and the cells were centrifuged for 2
313 minutes at 1200g. The PBMCs were then subjected to two washes with 50 mL of 3mM EDTA in
314 PBS with 2% FBS, each followed by a 2-minute centrifugation at 1200g. After cell counting, 5 x
315 10^7 PBMCs were resuspended in 8.5 mL of 3mM EDTA in PBS with 2% FBS. Monocytes were
316 subsequently isolated using the EasySep™ Human Monocyte Isolation Kit (StemCell
317 Technologies) in accordance with the manufacturer's protocol.
318
319 *Cell culture and Macrophage differentiation:*
320 The HC69.5 cells were cultured in Dulbecco's Modified Eagle Medium (DMEM) (ThermoFisher
321 Scientific, Cat. # 11965-118) supplemented with 10% fetal bovine serum (FBS) (Corning, Inc.,

322 Cat. #35-010-CV) and 10% Penicillin/1% Streptomycin (Fisher Scientific, Cat. #11548876) at
323 37°C with 5% CO2.
324
325 Freshly isolated monocytes were seeded in 12-well plates with 800 µL of differentiation medium
326 comprising ImmunoCult™-SF Macrophage Medium (StemCell Technologies) supplemented with
327 50 µg/mL human M-CSF (PeproTech) for macrophage differentiation. After 7 days, fully
328 differentiated cells were harvested using StemPro Accutase (Gibco) for downstream analysis.
329
330 *RNP preparation and cell nucleofection*
331 A mixture of 160 µM tracrRNA (IDT) and 160 µM crRNA (IDT) was incubated at 37°C for 30
332 minutes to generate guide RNA (gRNA) at a concentration of 80 µM. Subsequently, 4 µL of gRNA
333 was combined with 4 µL of purified SpCas9-NLS protein (QB3 core, Berkeley) at 40 µM and
334 incubated at 37°C for 15 minutes to form Cas9-Ribonucleoproteins (Cas9-RNPs). For
335 nucleofection, 8 µL of Cas9-RNPs were nucleofected per 1 x 10^6 HC69.5 cells or 1 x 10^6
336 monocytes, following the manufacturer's recommendations for a Lonza Nucleofector. The DN-
337 100 program with SF Buffer was employed for HC69.5 cells, while the DS-150 program with P3
338 buffer was utilized for monocytes.
339
340 *DNA Extraction, Sanger Sequencing and TIDE analysis.*
341 Cells were harvested, and genomic DNA was extracted from approximately 0.5 x 10^6 cells using
342 Qiagen Blood and Tissue Kits following the manufacturer's recommendations. The CRISPR-
343 targeted sequences were subsequently amplified using Phusion® High-Fidelity DNA Polymerase
344 (NEB). The primers used for the PCR were as follows: for *CXCR4*, 5'-
345 AGAGGAGTTAGCCAAGATGTGACTTTGAAACC-3' and 5'-
346 GGACAGGATGACAATACCAGGCAGGATAAGGCC-3'; for *CCR5*, 5'-

347 CTCACTATGCTGCCGCCCAGTG-3' and 5'-TCACCAGCCCACTTGAGTCCGT-3'; and for HIV
348 LTR, 5'-GCAAGTAGAAGAGGCCAATGAAGG-3' and 5'-TGCTAGAGATTTTCCACACTGACTA-
349 3'. The PCR products were purified using NucleoSpin Gel and PCR Clean-Up kits (Macherey-
350 Nagel) and subsequently sent for Sanger sequencing (ElimBio, California). AB1 sequencing files
351 were then analyzed using TIDE software.
352
353 *Flow Cytometry.*
354 For GFP measurement, HC69.5 cells were harvested and washed three times in PBS (Gibco).
355 Cells were resuspended at a concentration of 1 x 10^6 cells per mL and analyzed using an LSRII
356 flow cytometer.
357
358 For CCR5 flow cytometry, approximately 1 x 10^6 cells were washed three times with PBS and
359 resuspended in 100 µl of cell staining buffer. Cells were incubated with 5 µl of Human TruStain
360 FcX™ to block Fc receptors for 15 minutes, followed by APC anti-human CD195 (CCR5) (clone
361 J418F1, BioLegend) or 5 µl of the corresponding isotype control staining for 30 minutes.
362 Afterward, cells were washed three times with cell staining buffer and resuspended in 500 µl of
363 staining buffer. Samples were run on a BD LSR II flow cytometer (BD Biosciences).
364
365 For the phagocytosis assay, macrophages were washed and resuspended in serum-free IMDM
366 at a concentration of 1 x 10^6 cells/mL. A mixture of 100 µl of macrophages and 100 µl of
367 pHrodo™ Green E. coli BioParticles (Invitrogen, P35366) at 1 mg/mL was incubated for 45
368 minutes at 37°C. Phagocytosis was stopped by adding 900 µl of cold FACS buffer (PBS+2%
369 PBS). Cells were centrifuged at 500g for 5 minutes and washed with 1 mL of FACS buffer.
370 Subsequently, cells were resuspended in 100 µl of FACS Buffer and incubated with 5 µl of APC
371 anti-human CD14 for 30 minutes. After three washes with FACS Buffer, cells were resuspended

372 in 110 µl of FACS Buffer supplemented with 1 µM Propidium Iodide and analyzed on a FACS
373 Calibur Flow Cytometer (BD Biosciences).
374
375 Flow cytometry data were analyzed, and plots were generated using FlowJo (v10.9.0).
376
377 *Single-cell library preparation and sequencing*
378 Libraries were prepared following the manufacturer's recommendations for custom panels
379 (Mission Bio). Briefly, 300,000 HC69.5 or MDMs were encapsulated and barcoded using the
380 Mission Bio Tapestri single-cell sequencing platform. For the targeted PCR amplification step, the
381 conditions were as follows: incubation at 95°C for 10 minutes, followed by 20 cycles consisting of
382 30 seconds at 95°C, 10 seconds at 72°C, 6 minutes at 61°C, and 30 seconds at 72°C. Samples
383 were then incubated at 72°C for 2 minutes and kept at 4°C until the next step. All samples
384 exhibited DNA quantities within the expected yield range after PCR clean-up steps. Following
385 library PCR and clean-up, samples were pooled using the Tapestri Sample Quantification Tool,
386 and libraries were sequenced on an Illumina MiSeq using MiSeq Reagent Kit v2 (300-cycles) and
387 a 2x150bp reaction, following the manufacturer's recommendations.
388
389 *Bioinformatic analysis*
390 Sequences were analyzed using a custom pipeline to determine genome editing rates for both
391 the human and HIV genomes at each targeted amplicon in each cell. Briefly, the two 8bp cell
392 barcodes were read from individual sequencing reads and compared to the list of 768 possible
393 barcodes (v1 chemistry) with a custom Python script. Barcodes that were an exact match passed
394 the filter, and those with a Levenshtein distance of 1 away from a unique barcode in the allow list
395 were corrected to that barcode and also passed the filter. Reads that did not have both 8bp
396 barcodes passing the filter were discarded (overall barcode fail rate was 5.3-6.5%). All reads with

397 the same 16bp barcode were collected into individual files. Only barcodes with a minimum of 100
398 reads were processed using CRISPResso2 in batch mode[51]. The average number of aligned
399 reads per cell for each amplicon was then plotted. The percentage of reads modified, and the
400 modification state and frequency of CXCR4, CCR5, and HIV LTR for each cell and each amplicon
401 were analyzed using Python (v3.x) and R Studio (v2023.06.2+561). Briefly, each mutation (indel)
402 was characterized by its size. Cells with fewer than 5 reads for each CRISPR-targeted amplicon
403 were filtered out, and the overall frequency for each indel size and total editing efficiency were
404 plotted.
405
406 For the heterozygosity analysis, amplicons corresponding to targeted sites in CXCR4 and CCR5
407 genes and HIV-LTR were labeled with their mutational state (Wild Type or Mutated), and the
408 frequency of each event was recorded. For each amplicon, each cell was classified into one of
409 three classes: WT/WT, WT/Mut, or Mut/Mut based on the overall percentage of reads with indels
410 in a given cell. Cells with < 20% modified reads were considered WT/WT. Cells with ≥ 20% and
411 < 80% modified reads were considered heterozygous WT/Mut. Cells with ≥ 80% mutated reads
412 were classified as homozygous Mut/Mut. A heatmap has been plotted summarizing these results
413 where each line represents one cell.
414
415 *Statistical analysis*
416 The results presented were analyzed with GraphPad Prism v10 (GraphPad Software,
417 SanDiego, CA, USA). Information on specific tests that were used are described in the Results
418 section.
419
420 **Acknowledgments**

The authors would like to acknowledge Drs. Li Du, Prerna Dabral, and Hannah S. Schwarzer-Sperber at Vitalant Research Institute, and Drs. Robert Durruthy-Durruthy and Shu Wang at Mission Bio for guidance and support in data analysis.

This research was supported by the NIH-funded UCSF-Bay Area Center for AIDS Research (P30 AI027763) specific mechanism: Gilead funded HIV Mentored Scientist award at the amfAR Institute for HIV Cure Research (Vitalant Subaward 12194sc).

Author Contributions

M.S.B., L.R.C. and S.K.P. initiated the project and designed the experiments. M.S.B., K.A.R. and S.D. performed the bulk sequencing and M.S.B. analyzed the data. M.S.B., K.A.R. L.R.C. performed the single cell sequencing. Z.Y.D. and M.S.B. analyzed the sc-seq data. C.D.B. performed the phagocytosis assay. M.S.B. and S.K.P. prepared the manuscript and M.S.B., P.B. and S.K.P. jointly supervised the work.

Declaration of interests

There is no conflict of interest regarding the publication of this article.

References

1. HIV and AIDS. https://www.who.int/news-room/fact-sheets/detail/hiv-aids.

2. Eisinger, R. W., Dieffenbach, C. W. & Fauci, A. S. HIV Viral Load and Transmissibility of HIV Infection: Undetectable Equals Untransmittable. *JAMA* **321**, 451–452 (2019).

3. Ho, Y.-C. *et al.* Replication-competent noninduced proviruses in the latent reservoir increase barrier to HIV-1 cure. *Cell* **155**, 540–551 (2013).

4. Abana, C. Z.-Y., Lamptey, H., Bonney, E. Y. & Kyei, G. B. HIV cure strategies: which ones are appropriate for Africa? *Cell Mol Life Sci* **79**, 400 (2022).

448 5. Ismail, S. D. *et al.* Addressing an HIV cure in LMIC. *Retrovirology* **18**, 21 (2021).

449 6. Deeks, S. G. HIV: Shock and kill. *Nature* **487**, 439–440 (2012).

450 7. Vansant, G., Bruggemans, A., Janssens, J. & Debyser, Z. Block-And-Lock Strategies to
451 Cure HIV Infection. *Viruses* **12**, 84 (2020).

452 8. Gonzalez-Cao, M., Martinez-Picado, J., Karachaliou, N., Rosell, R. & Meyerhans, A.
453 Cancer immunotherapy of patients with HIV infection. *Clin Transl Oncol* **21**, 713–720 (2019).

454 9. Hütter, G. *et al.* Long-term control of HIV by CCR5 Delta32/Delta32 stem-cell
455 transplantation. *N Engl J Med* **360**, 692–698 (2009).

456 10. Gupta, R. K. *et al.* HIV-1 remission following CCR5Δ32/Δ32 haematopoietic stem-cell
457 transplantation. *Nature* **568**, 244–248 (2019).

458 11. Jensen, B.-E. O. *et al.* In-depth virological and immunological characterization of HIV-1
459 cure after CCR5Δ32/Δ32 allogeneic hematopoietic stem cell transplantation. *Nat Med* **29**, 583–
460 587 (2023).

461 12. Manjunath, N., Yi, G., Dang, Y. & Shankar, P. Newer gene editing technologies toward
462 HIV gene therapy. *Viruses* **5**, 2748–2766 (2013).

463 13. Khalili, K., Kaminski, R., Gordon, J., Cosentino, L. & Hu, W. Genome editing strategies:
464 potential tools for eradicating HIV-1/AIDS. *J Neurovirol* **21**, 310–321 (2015).

465 14. Hütter, G. *et al.* CCR5 Targeted Cell Therapy for HIV and Prevention of Viral Escape.
466 *Viruses* **7**, 4186–4203 (2015).

467 15. Jiang, F. & Doudna, J. A. CRISPR-Cas9 Structures and Mechanisms. *Annu Rev*
468 *Biophys* **46**, 505–529 (2017).

469 16. Chavez, L. R. *et al.* Durable Control of HIV-1 Using a Staphylococcus aureus Cas9-
470 Expressing Lentivirus Co-Targeting Viral Latency and Host Susceptibility. 2020.08.10.243329
471 Preprint at https://doi.org/10.1101/2020.08.10.243329 (2020).

472 17. Yin, C. *et al.* In Vivo Excision of HIV-1 Provirus by saCas9 and Multiplex Single-Guide
473 RNAs in Animal Models. *Molecular Therapy* **25**, 1168–1186 (2017).

474 18. Yin, C. *et al.* Functional screening of guide RNAs targeting the regulatory and structural
475 HIV-1 viral genome for a cure of AIDS. *AIDS* **30**, 1163–1174 (2016).

476 19. Kaminski, R. *et al.* Excision of HIV-1 DNA by gene editing: a proof-of-concept in vivo
477 study. *Gene Ther* **23**, 696 (2016).

478 20. Liao, H.-K. *et al.* Use of the CRISPR/Cas9 system as an intracellular defense against
479 HIV-1 infection in human cells. *Nat Commun* **6**, 6413 (2015).

480 21. Kaminski, R. *et al.* Elimination of HIV-1 Genomes from Human T-lymphoid Cells by
481 CRISPR/Cas9 Gene Editing. *Sci Rep* **6**, 22555 (2016).

482 22. RNA-directed gene editing specifically eradicates latent and prevents new HIV-1
483 infection | PNAS. https://www.pnas.org/doi/10.1073/pnas.1405186111.

484 23. Hou, P. *et al.* Genome editing of CXCR4 by CRISPR/cas9 confers cells resistant to HIV-
485 1 infection. *Sci Rep* **5**, 15577 (2015).

486 24. Ye, L. *et al.* Seamless modification of wild-type induced pluripotent stem cells to the
487 natural CCR5Δ32 mutation confers resistance to HIV infection. *Proceedings of the National*
488 *Academy of Sciences* **111**, 9591–9596 (2014).

489 25. Wang, W. *et al.* CCR5 Gene Disruption via Lentiviral Vectors Expressing Cas9 and
490 Single Guided RNA Renders Cells Resistant to HIV-1 Infection. *PLOS ONE* **9**, e115987 (2014).

491 26. Dash, P. K. *et al.* Sequential LASER ART and CRISPR Treatments Eliminate HIV-1 in a
492 Subset of Infected Humanized Mice. *Nat Commun* **10**, 2753 (2019).

493 27. Yin, C. *et al.* In Vivo Excision of HIV-1 Provirus by saCas9 and Multiplex Single-Guide
494 RNAs in Animal Models. *Mol Ther* **25**, 1168–1186 (2017).

495 28. Kaminski, R. *et al.* Excision of HIV-1 DNA by gene editing: a proof-of-concept in vivo
496 study. *Gene Ther* **23**, 690–695 (2016).

497 29. Bella, R. *et al.* Removal of HIV DNA by CRISPR from Patient Blood Engrafts in
498 Humanized Mice. *Mol Ther Nucleic Acids* **12**, 275–282 (2018).

499 30. Mancuso, P. *et al.* CRISPR based editing of SIV proviral DNA in ART treated non-
500 human primates. *Nat Commun* **11**, 6065 (2020).

501 31. Hiatt, J. *et al.* Efficient generation of isogenic primary human myeloid cells using
502 CRISPR-Cas9 ribonucleoproteins. *Cell Rep* **35**, 109105 (2021).

503 32. Yaseen, M. M., Abuharfeil, N. M., Alqudah, M. A. & Yaseen, M. M. Mechanisms and
504 Factors That Drive Extensive Human Immunodeficiency Virus Type-1 Hypervariability: An
505 Overview. *Viral Immunol* **30**, 708–726 (2017).

506 33. Johnson, M. M., Jones, C. E. & Clark, D. N. The Effect of Treatment-Associated
507 Mutations on HIV Replication and Transmission Cycles. *Viruses* **15**, 107 (2022).

508 34. Wang, G., Zhao, N., Berkhout, B. & Das, A. T. CRISPR-Cas9 Can Inhibit HIV-1
509 Replication but NHEJ Repair Facilitates Virus Escape. *Mol Ther* **24**, 522–526 (2016).

510 35. De Silva Feelixge, H. S. *et al.* Detection of treatment-resistant infectious HIV after
511 genome-directed antiviral endonuclease therapy. *Antiviral Res* **126**, 90–98 (2016).

512 36. Anti-HIV-1 potency of the CRISPR/Cas9 system insufficient to fully inhibit viral
513 replication - Ueda - 2016 - Microbiology and Immunology - Wiley Online Library.
514 https://onlinelibrary.wiley.com/doi/full/10.1111/1348-0421.12395.

515 37. Wang, Z. *et al.* CRISPR/Cas9-Derived Mutations Both Inhibit HIV-1 Replication and
516 Accelerate Viral Escape. *Cell Rep* **15**, 481–489 (2016).

517 38. Yoder, K. E. & Bundschuh, R. Host Double Strand Break Repair Generates HIV-1
518 Strains Resistant to CRISPR/Cas9. *Sci Rep* **6**, 29530 (2016).

519 39. Sei, S. *et al.* Protective effect of CCR5 delta 32 heterozygosity is restricted by SDF-1

520 genotype in children with HIV-1 infection. *AIDS* **15**, 1343–1352 (2001).

521 40. Trecarichi, E. M. *et al.* Partial protective effect of CCR5-Delta 32 heterozygosity in a
522 cohort of heterosexual Italian HIV-1 exposed uninfected individuals. *AIDS Res Ther* **3**, 22
523 (2006).

524 41. Huang, Y. *et al.* The role of a mutant CCR5 allele in HIV-1 transmission and disease
525 progression. *Nat Med* **2**, 1240–1243 (1996).

526 42. Bennett, E. P. *et al.* INDEL detection, the 'Achilles heel' of precise genome editing: a
527 survey of methods for accurate profiling of gene editing induced indels. *Nucleic Acids Research*
528 **48**, 11958–11981 (2020).

529 43. Hiatt, J. *et al.* A functional map of HIV-host interactions in primary human T cells. *Nat*
530 *Commun* **13**, 1752 (2022).

531 44. Burdo, T. H. *et al.* Preclinical safety and biodistribution of CRISPR targeting SIV in non-
532 human primates. *Gene Ther* 1–10 (2023) doi:10.1038/s41434-023-00410-4.

533 45. Garcia-Mesa, Y. *et al.* Immortalization of primary microglia: a new platform to study HIV
534 regulation in the central nervous system. *J Neurovirol* **23**, 47–66 (2017).

535 46. Veenhuis, R. T. *et al.* Monocyte-derived macrophages contain persistent latent HIV
536 reservoirs. *Nat Microbiol* 1–12 (2023) doi:10.1038/s41564-023-01349-3.

537 47. Chakrabarti, A. M. *et al.* Target-Specific Precision of CRISPR-Mediated Genome Editing.
538 *Molecular Cell* **73**, 699-713.e6 (2019).

539 48. Regoes, R. R. & Bonhoeffer, S. The HIV coreceptor switch: a population dynamical
540 perspective. *Trends Microbiol* **13**, 269–277 (2005).

541 49. ten Hacken, E. *et al.* High throughput single-cell detection of multiplex CRISPR-edited
542 gene modifications. *Genome Biology* **21**, 266 (2020).

543 50. Leitner, T. *et al.* Analysis of heterogeneous viral populations by direct DNA sequencing.
544 *Biotechniques* **15**, 120–127 (1993).

545 51. Clement, K. *et al.* CRISPResso2 provides accurate and rapid genome editing sequence
546 analysis. *Nat Biotechnol* **37**, 224–226 (2019).

547

548

549

550

551 **Figures and Tables**

552

553 **Figure 1. Map of primer binding sites across the HIV genome.** Blue and red bars represent
554 forward and reverse sequencing primers, respectively. A total of 36 primer pairs were employed
555 to achieve near-complete coverage of the HIV genome. Nucleotide coordinates corresponding to
556 each primer pair are provided below the bars.

557

558 **Figure 2. Schematic of anti-HIV gene editing workflow.** A) RNP complexes were generated
559 using guides targeting the LTR, CXCR4, or CCR5 loci. The resulting complexes were pooled and
560 delivered to HC69.5 cells utilizing a Lonza 4D-Nucleofector. After 48 hours of culture, cells were
561 harvested for downstream analyses as indicated. B) PBMCs were isolated from whole blood
562 obtained from healthy donors. Monocytes were then isolated using a negative selection antibody
563 cocktail. Simultaneously, CXCR4 and CCR5 targeting guides were generated and complexed
564 with purified Cas9 protein to form CXCR4 and CCR5 targeting Cas9-RNPs. These RNPs were
565 pooled and delivered to freshly isolated monocytes using a Lonza 4-D Nucleofector. Following
566 stimulation with M-CSF for 7 days, MDMs were polarized. Harvested cells underwent DNA
567 extraction for PCR amplification and Sanger sequencing, scDNA-seq library preparation, flow
568 cytometry, and phagocytosis assays.

569

570 **Figure 3. Comparison of inferred gene editing efficiencies between single-cell and bulk**
571 **Sanger sequencing approaches.** Inferred editing efficiency comparison between bulk TIDE
572 analysis (blue), bulk CRISPResso2 (red) and single cell CRISPResso2 (green) methods in
573 HC69.5 (A) or primary MDMs (B). Editing efficiencies are indicated above the bars for each
574 method and each target, expressed as percentages. (C) Flow cytometry on HC69.5 cells

575 nucleofected with scrambled guide RNPs (control) or CXCR4, CCR5 and HIV LTR-targeting
576 RNPs.
577
578 **Figure 4. Comparison of inferred indel spectra between single-cell and bulk Sanger**
579 **sequencing approaches.** The sum of the number of peaks inferred using TIDE (green) or
580 single-cell analysis (blue) were plotted for each target in each cell type. The target names and
581 cell types are labeled along the x-axis, with the number of detected indel sizes indicated on the
582 y-axis. Statistical significance was determined using a paired t-test (*$p<0.05$)
583
584 **Figure 5. Heatmap visualization of multi-site gene editing within individual cells.** Each line
585 in the heatmap represents one cell, with the shade of green indicating the editing frequency for
586 each target. (A & B) Detailed view of the editing per cell and per loci analyzed in (A) HC69.5
587 cells and (B) MDMs. Editing values above 0.8 indicate bi-allelic editing, between 0.2 and 0.8
588 indicate mono-allelic editing, and below 0.2 indicate no editing. (C & D) Discretized editing
589 heatmaps for (C) HC69.5 cells and (D) MDMs. Biallelic editing is represented in dark green,
590 monoallelic editing in light green and unedited in pale green. Numbers indicate the number of
591 cells in each group, with cell counts below 100 excluded for clarity.
592
593 **Figure 6. Interdependency of gene editing events.** Expected number of cells harboring no
594 editing, mono editing, or co-editing between CXCR4 and CCR5 loci (A) or between CXCR4 and
595 CCR5 alleles (B & C) have been calculated and plotted (green) and compared to observed
596 values (blue). Statistical significance was determined using Chi-square tests, comparing
597 observed values to expected values (***$P < 0.001$, ****$P < 0.0001$).
598

599 **Supplementary Figure 1. Amplicon coverage across host and viral genome targets.** (A)
600 Read coverage for each amplicon in the HC69.5 cell line obtained through the CRISPResso2
601 pipeline are plotted. The amplicon names are labeled along the x-axis, with the average reads
602 per cell plotted on the y-axis. A gap in reads observed between AMP6 and AMP21 corresponds
603 to the deletion identified in the HC69.5 HIV provirus. (B) Coverage across the HIV genome and
604 host genes in the J-Lat 11.1 cell line. (C) Host gene coverage in HC69.5 cells. The amplicon name
605 is indicated on the x-axis and the average reads per cell is indicated in the y-axis.
606
607 **Supplementary Figure 2. Gene editing workflow does not impede the functional activity**
608 **of primary MDMs.** Cells were incubated for 45 minutes with fluorescent bioparticles to measure
609 phagocytosis and analyzed by flow cytometry. The gating strategy is indicated on the left and
610 the frequency of CD14+ Bioparticles+ cells compared to the total of CD14+ cells and the mean
611 fluorescent intensity (MFI) for control cells and knocked out cells is indicated in the table on the
612 right.
613
614 **Supplementary Table 1. Complete list of targets in scDNA-seq panel.**

Figure 1

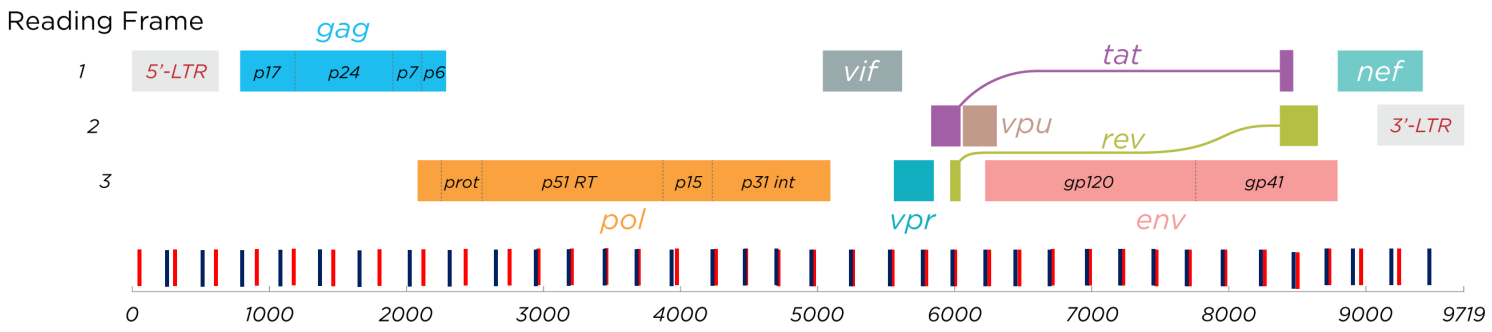

| : 5' primers

| : 3' primers

Figure 2

A.

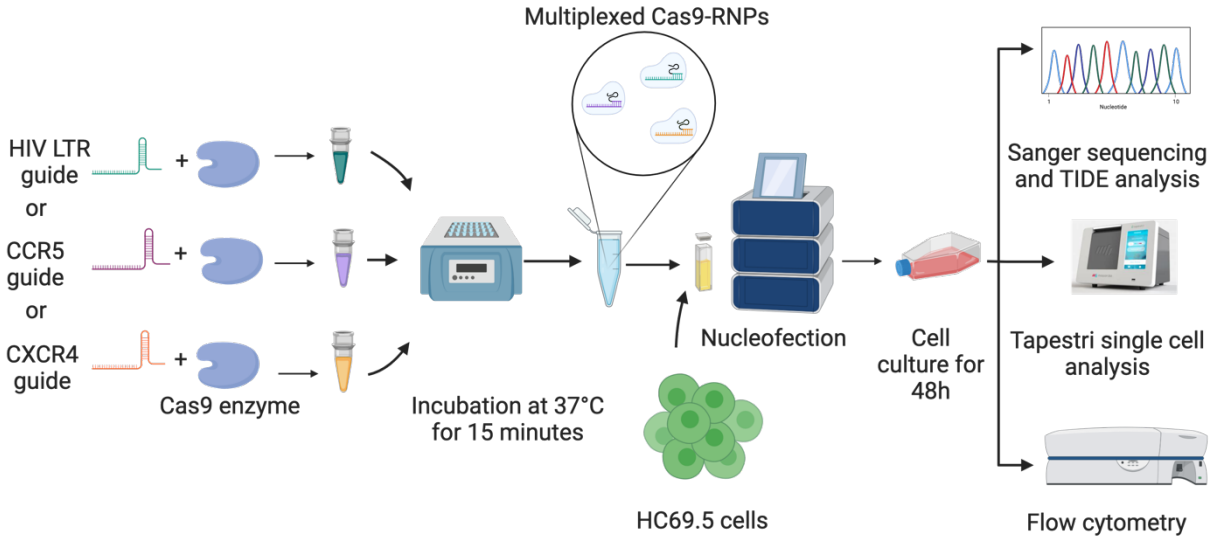
Multiplexed Cas9-RNPs
HIV LTR guide
or
CCR5 guide
or
CXCR4 guide
Cas9 enzyme
Incubation at 37°C for 15 minutes
Nucleofection
HC69.5 cells
Cell culture for 48h
Sanger sequencing and TIDE analysis
Tapestri single cell analysis
Flow cytometry

B.

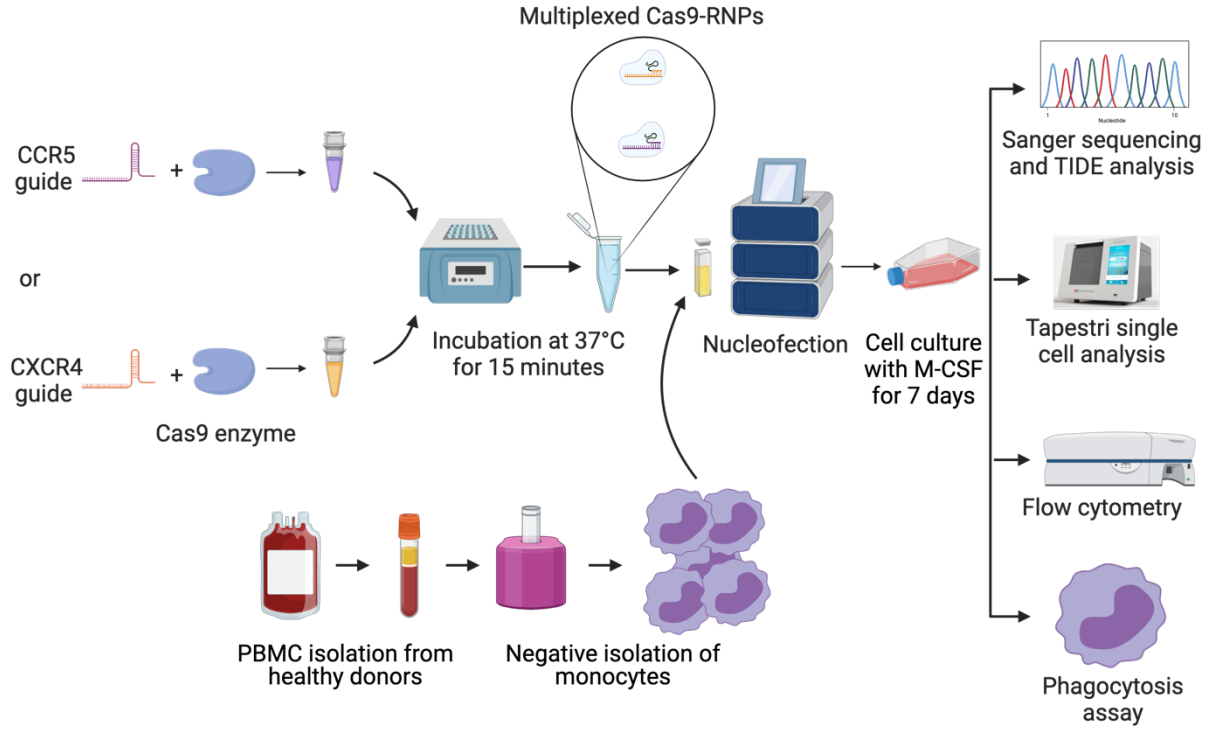
Multiplexed Cas9-RNPs
CCR5 guide
or
CXCR4 guide
Cas9 enzyme
Incubation at 37°C for 15 minutes
Nucleofection
Cell culture with M-CSF for 7 days
Sanger sequencing and TIDE analysis
Tapestri single cell analysis
Flow cytometry
Phagocytosis assay
PBMC isolation from healthy donors
Negative isolation of monocytes

Figure 3

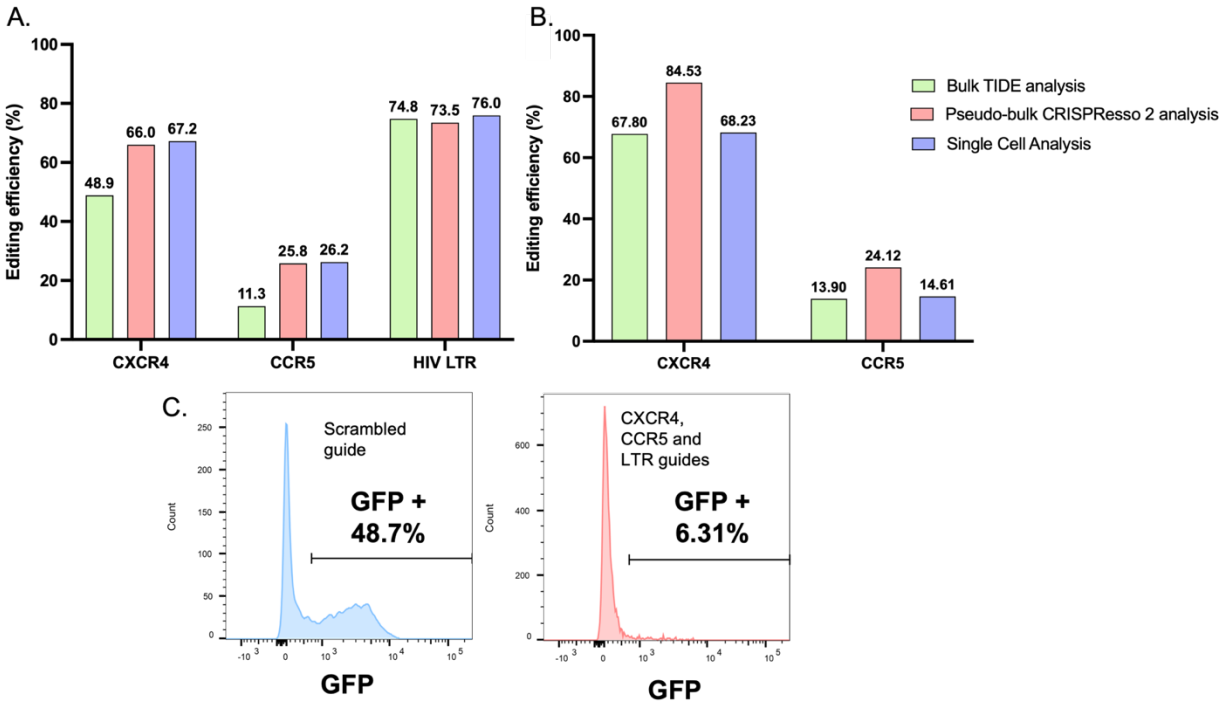
A.
Editing efficiency (%)
100
80
60
40
20
0
48.9
66.0
67.2
11.3
25.8
26.2
74.8
73.5
76.0
CXCR4
CCR5
HIV LTR
B.
Editing efficiency (%)
67.80
84.53
68.23
13.90
24.12
14.61
CXCR4
CCR5
Bulk TIDE analysis
Pseudo-bulk CRISPResso 2 analysis
Single Cell Analysis
C.
Scrambled guide
GFP +
48.7%
Count
GFP
CXCR4, CCR5 and LTR guides
GFP +
6.31%
Count
GFP

Figure 4.

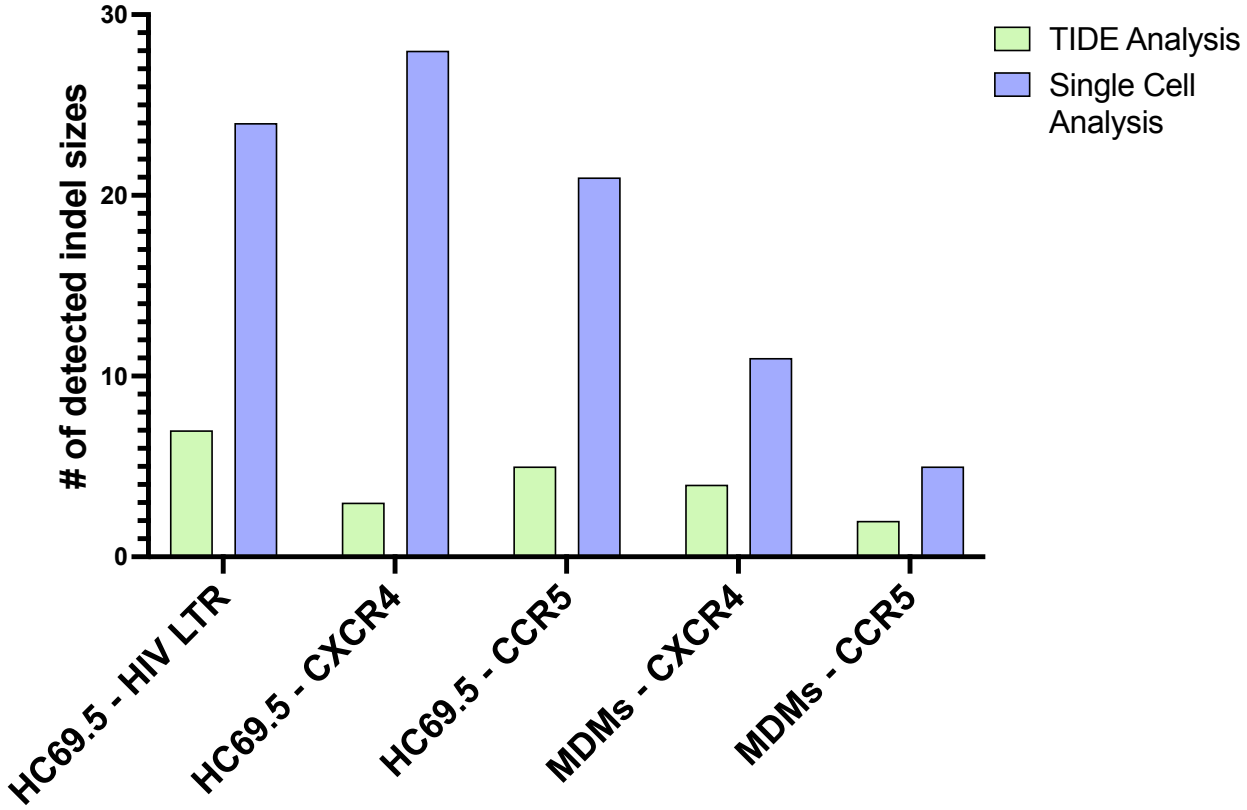
30
20
10
0
# of detected indel sizes
TIDE Analysis
Single Cell Analysis
HC69.5 - HIV LTR
HC69.5 - CXCR4
HC69.5 - CCR5
MDMs - CXCR4
MDMs - CCR5

Figure 5

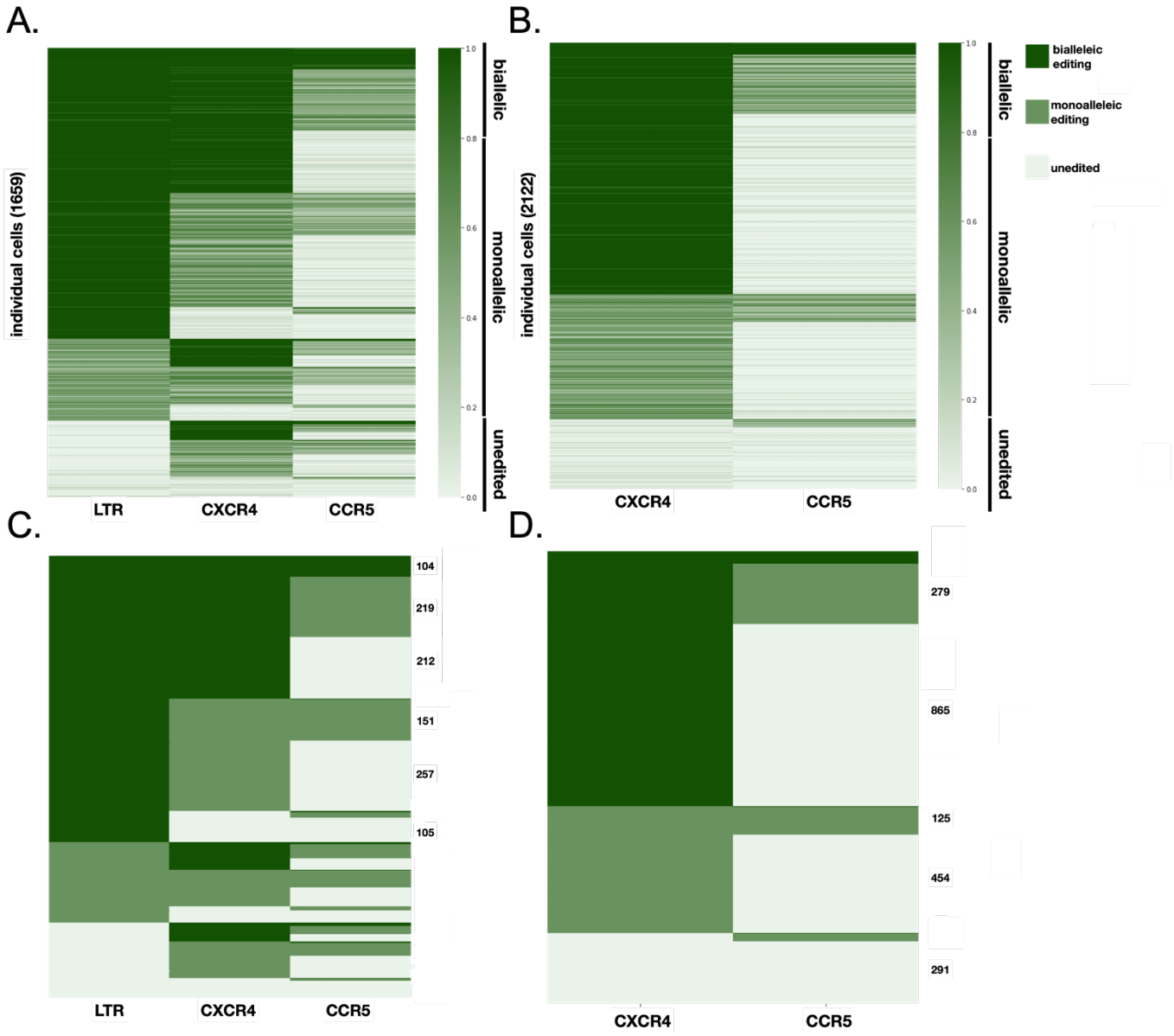
A.
individual cells (1659)
LTR
CXCR4
CCR5
biallelic
monoallelic
unedited
B.
individual cells (2122)
CXCR4
CCR5
biallelic
monoallelic
unedited
bialleleic editing
monoalleleic editing
unedited
C.
104
219
212
151
257
105
LTR
CXCR4
CCR5
D.
279
865
125
454
291
CXCR4
CCR5

Figure 6

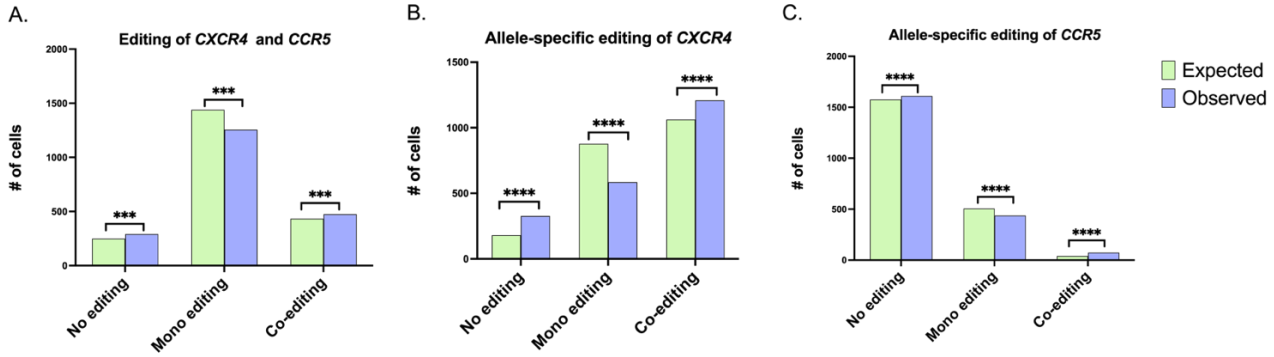
A.
Editing of CXCR4 and CCR5
# of cells
2000
1500
1000
500
0
***
***
***
No editing
Mono editing
Co-editing
B.
Allele-specific editing of CXCR4
# of cells
1500
1000
500
0
****
****
****
No editing
Mono editing
Co-editing
C.
Allele-specific editing of CCR5
# of cells
2000
1500
1000
500
0
****
****
****
No editing
Mono editing
Co-editing
Expected
Observed

Supplementary Table 1

Ampcon ID	Chromosome	Forward Primer Amplicon start coordinates	Amplicon end coordinates	Reverse Primer coordinates	Forward Primr	Reverse Primer Sequence	Amplicon Sequence	Target
BSRI_HV_AMP1	KD3455.1	7	30	180	201	GGCTAATTCACGCTGGTGTTGTTGT	GGCTAATTCACTCCAACGAAGACAAGATATCCTT	HV_1_HXB2
BSRI_HV_AMP2	KD3455.1	206	225	402	420	ACACCCTGTGGATCTGAGCGCTCGCCACT	ACACCCTGTGAGCCTGCATGGATGACCCG	HV_1_HXB2
BSRI_HV_AMP3	KD3455.1	441	462	678	696	TTTTGCCTGTATCCTGCGTCGAGAGAGCT	TTTTGCCTGTACTGGGTCTCTCTGGTTAGACCAGA	HV_1_HXB2
BSRI_HV_AMP4	KD3455.1	738	756	989	1012	CGACTGCTGTGATGTCTTCTGATCCTGTCTGAAGG	CGACTGGTGAGTACGGCGAAAATTTTGACTAGCGG	HV_1_HXB2
BSRI_HV_AMP5	KD3455.1	1075	1099	1288	1315	GACACCAAGGAATTTAGCAAAACATGGGTATCACTT	GACACCAAGGAAGCTTTAGACAAGATAGAGGAH	HV_1_HXB2
BSRI_HV_AMP6	KD3455.1	1364	1383	1615	1638	GGGGGACATCACAGAATGCTGGTAGGGCTATACA	GGGGGACATCAAGCAGCCATGCAAATGTTAAAAG	HV_1_HXB2
BSRI_HV_AMP7	KD3455.1	1765	1794	1989	2009	GCGAACCAGATTGTAAAGACATTTTTAAAAGCATT	GCGAACCAGATTGTAAAGACATTTTTAAAAGCATT	HV_1_HXB2
BSRI_HV_AMP8	KD3455.1	2153	2173	2394	2419	CAACAGCCCCACCAAGAAGAGAGCTTCAGGTCTGG	CAACAGCCCCACCAGAAGAGAGCTTCAGGTCTGG	HV_1_HXB2
BSRI_HV_AMP9	KD3455.1	2420	2452	2668	2694	AAGACAGTATGATCAGATACTCATAGAAATCTGTH	AAGACAGTATGATCAGATACTCATAGAAATCTGTH	HV_1_HXB2
BSRI_HV_AMP10	KD3455.1	2695	2719	2913	2939	AAATTGGGGCCATGGCAATGCAATACAATACTCCAGTH	AAATTGGGGCCATGGCAATGCAATACAATACTCCAGTH	HV_1_HXB2
BSRI_HV_AMP11	KD3455.1	2940	2968	3160	3183	ACCATACCTAGACCTCAACAGATGTTGTCTCAGC	ACCATACCTAGTATAAACAATGAGACACCAGGGA	HV_1_HXB2
BSRI_HV_AMP12	KD3455.1	3184	3204	3399	3429	GGGGGACTTACGTATTACTTCTGTTAGTGCTTTGGTTCCTC	GGGGGACTTACCACACCAGACAAAAAAACATCAGAA	HV_1_HXB2
BSRI_HV_AMP13	KD3455.1	3430	3454	3674	3609	CACTAACAGAAGAAGCAGGCATGACTATCTGTGGT	CACTAACAGAAGAAGCAGGCATGACTGTGCAGATH	HV_1_HXB2
BSRI_HV_AMP14	KD3455.1	3702	3727	3949	3973	AAGACTCCTAATTGATTTGTTGTGTCAGTTAGGGTG	AAGACTCCTAAATTTAAACTGGCCATACAAAAGGA	HV_1_HXB2
BSRI_HV_AMP15	KD3455.1	3978	4005	4206	4232	ACTGAGTTAAGAATAGTACTTTCCTGATTCCAGCAC	ACTGAGTTACAAGCAATTTATCTAGCTTTGCAGGH	HV_1_HXB2
BSRI_HV_AMP16	KD3455.1	4233	4259	4454	4478	TTAGATGGAATATCATCCATTGCAGTCTGCAACTGC	TTAGATGGAATAGATAAGGCCCAAGATGAACATH	HV_1_HXB2
BSRI_HV_AMP17	KD3455.1	4479	4504	4706	4734	ATAGAAGCAGAAGCTGATCCTTCACCTGTCATAATTT	ATAGAAGCAGAAGTTATTCAGCGAAAACAGGGTH	HV_1_HXB2
BSRI_HV_AMP18	KD3455.1	4735	4760	4963	4990	CTGAACATCTTTATCTTGTATTACTACTGCCCCTTCA	CTGAACATCTTAAGACAGCAGTACAAATGGCAGTH	HV_1_HXB2
BSRI_HV_AMP19	KD3455.1	4991	5018	5213	5237	TAGTGACATAATAACCAATCATCAGCATCCCCTAGT	TAGTGACATAAAAGTAGTGCAAGAAGAAAAAGCH	HV_1_HXB2
BSRI_HV_AMP20	KD3455.1	5238	5263	5451	5481	AACAACATATTGTAGAGATCTCCTGTTGCCATCCTT	AACAACATTTGTAAATGTGGAAGCAGGAGAAAGH	HV_1_HXB2
BSRI_HV_AMP21	KD3455.1	5485	5509	5709	5729	GCACTAGCAG CACTCCTGCCCAAGTATCCC	GCACTAGCAGCATTAATAACACCAAAAAAGATAAH	HV_1_HXB2
BSRI_HV_AMP22	KD3455.1	5730	5756	5958	5977	GAAGCCATAA CCTGCCATAGGAGATGCCT	GAAGCCATAATAAGAATTCTGGAACAACTGCTGTH	HV_1_HXB2
BSRI_HV_AMP23	KD3455.1	5978	5996	6198	6222	AAGAAGCCGGCCACTGCTTTCCTCCTCCTCCTCATT	AAGAAGCCGGAACACGCAGGAAGAGCTCATGAG	HV_1_HXB2
BSRI_HV_AMP24	KD3455.1	6223	6252	6447	6467	CAATGAGAGT TGGGTTGGGGCTGTGTGGGTA	CAATGAGAGTGAAGGAGAAATATCAGCACTTGCTH	HV_1_HXB2
BSRI_HV_AMP25	KD3455.1	6468	6496	6689	6713	CAAGAAGTAGTATTGGTAAATGTGACAGAAATTH	CAAGAAGTAGTATTGGTAAATGTGACAGAAATTH	HV_1_HXB2
BSRI_HV_AMP26	KD3455.1	6714	6737	6934	6957	AGCATAAGAGCTGTGCTGATGAATTTGGTGGTGT	AGCATAAGAGCAAGAAGAATATGCAGTGTGTH	HV_1_HXB2
BSRI_HV_AMP27	KD3455.1	6958	6983	7188	7216	TACAATGTACATAATGTTGTCTGTCTCATATTTCCTATTT	TACAATGTACACATGGAATTAGGCCAGTAGTATGTH	HV_1_HXB2
BSRI_HV_AMP28	KD3455.1	7217	7247	7434	7461	TAACATTAGTAGTGTCACTTCCTTCAGTGTTATTTGACC	TAACATTAGTAGAGCAAATGGAATAACACTTTAH	HV_1_HXB2
BSRI_HV_AMP29	KD3455.1	7462	7483	7693	7717	CAATCACCTGCCATCGCCAGTAAAACAAATTATAH	CAATCACCTGCCATCGCCAGTAAAACAAATTATAH	HV_1_HXB2
BSRI_HV_AMP30	KD3455.1	7718	7740	7941	7960	CACCAAGGCAA CTTGCCTGGAGCTGCTTGA	CACCAAGGCAAAGAGAAGAGTGGTGCAGAGAGH	HV_1_HXB2
BSRI_HV_AMP31	KD3455.1	7961	7984	8176	8205	AATCCTGGCTGTGGAAAGATACCTAAAAGATCAA	AATCCTGGCTGTGGAAAGATACCTAAAAGATCAA	HV_1_HXB2
BSRI_HV_AMP32	KD3455.1	8206	8233	8430	8452	TGGAATTAGATAAATGTGGCAAGTTTGTTGGAATTT	TGGAATTAGATAAATGTGGCAAGTTTGTGGAATTH	HV_1_HXB2
BSRI_HV_AMP33	KD3455.1	8453	8478	8675	8696	CAGATCCATTC CTCAGCTACTGCTATGGCTGT	CAGATCCATTCGATTAGTGAACGGATCCTTGGCAH	HV_1_HXB2
BSRI_HV_AMP34	KD3455.1	8697	8726	8919	8942	GGGACAGATAGTGCTGATTTGCTACTTGTGATTGC	GGGACAGATAGGGTTATAGAAGTAGTACAAGGAH	HV_1_HXB2
BSRI_HV_AMP35	KD3455.1	8972	8992	9223	9245	AAGCACAAGAGGGCTCACATGGTCATACAGCTTGT	AAGCACAAGAGGAGGAGGAGGTGGGTTTTCCAGH	HV_1_HXB2
BSRI_HV_AMP36	KD3455.1	9250	9277	9494	9516	AAGATAGAAGAGGCCATAAAGCAGGACTGCAGGGCT	AAGATAGAAGAGGCCATAAAGCAGGACAGAACAC	HV_1_HXB2
BSRI_HV_AMP37	chr1	19565711	19565737	19565927	19565949	TTCTCAATACT TCCCTCTGCTTCTTAAATGCCTG	TTCTCAATACTCACCACTTCATTCCGCACAGCCATG	EMC1-01
BSRI_HV_AMP38	chr1	19567436	19567463	19567630	19567656	TCCCCAGTACAAGAAATCATAGCTCCCCCAATGCA	TCCCCAGTACAAGAAATCATAGCTCCCCCAATGCA	EMC1-02
BSRI_HV_AMP39	chr1	19570370	19570392	19570549	19570574	TGTACAGATGCTATTTAGGCTCTTCTGGGTTGCCA	TGTACAGATGCAAGGAAGCGAAGGAATGGGACAGG	EMC1-03
BSRI_HV_AMP40	chr1	109771939	109771964	109772141	109772163	ATCTTTAGAGCAGAAGGTTTGGGCAACCGAA	ATCTTTAGAGCACAACAGGGTTAGGGCAACCGAA	SARS-02
BSRI_HV_AMP41	chr1	109778957	109778982	109779156	109779179	TTAGCCTTCTGGAATACCATCCCTCCTTGATGAATT	TTAGCCTTCTGAAATACCATCCCTCCTTGATGAATT	SARS-03
BSRI_HV_AMP42	chr1	109779821	109779842	109780041	109780065	ATGAGAGTTGCAAGGGACCACTTCCCCCTCGGGACCT	ATGAGAGTTGCAAGGGACCACTTCCCCCTCGGGACCT	SARS-01
BSRI_HV_AMP43	chr1	115267786	115267813	115267990	115268016	CATCCTTTATC CTGCCTGTTATCTGTTGATGTTTATGG	CATCCTTTATCTCCCACTTAAAAGCACAGGCTGAATCSDE1-02	
BSRI_HV_AMP44	chr1	115275282	115275304	115275498	115275525	TGCTCGCTCTATTGTCAGCTGGGTCTGTTGTAAA	TGCTCGCTCTAATTTGTCAGCTGGGTCTGTTGAAA	CSDE1-03
BSRI_HV_AMP45	chr1	115282308	115282336	115282492	115282519	ATTACCTTCATA TACCTCTAATAAGATGAGCTTGATCAAACC	ATTACCTTCATATTTATTAAGTCTGGCAGGTTGCCATT	CSDE1-01
BSRI_HV_AMP46	chr2	27355030	27355051	27355214	27355237	CCAGGCAGGGATCCTTTCCAAGGTCAACTGCCCAG	CCAGGCAGGACTCCTTTCCAAGGTCAACTGCCCAG	PRE8-03
BSRI_HV_AMP47	chr2	27355657	27355680	27355835	27355856	CATAAGCACCTCTCTCTCCTTTCTCCATCCTCTCCCT	CATAAGCACCTCCTCTCTCCTTTCTCCATCCTCTCCCT	PRE8-01
BSRI_HV_AMP48	chr2	27356319	27356342	27356516	27356538	AGACCCACTCTCACTCCCATGGACAGAGAACAC	AGACCCACTCTCACTCCCATGGACAGAGAACAC	PRE8-02
BSRI_HV_AMP49	chr2	47693660	47693692	47693906	47693934	CTGGTTAGATAATAATTGTGAGTATGTTGTCATA	CTGGTTAGATAATAATTGTGAGTATGTTGTCATA	MSH2-03
BSRI_HV_AMP50	chr2	47703535	47703558	47703757	47703784	ATTCGACAAACTGGGGTGATAGTACTCATGGGCCC	ATTCGACAAACTGGGGTGATAGTACTCATGGGCCC	MSH2-02
BSRI_HV_AMP51	chr2	47705395	47705420	47705616	47705644	TAATTATGTGCTAAAGGATAGTTAAGGTCTTCAGTGG	TAATTATGTGCTAAAGGATAGTTAAGGTCTTCAGTGG	MSH2-01
BSRI_HV_AMP52	chr2	74689449	74689471	74689655	74689686	TATCTGCTCCCGGTATTGCCAGACATCGGGGGT	TATCTGCTCCCTCCAATCCAGCCATCAGCATTTAG	MOGS-02;MOGS-03
BSRI_HV_AMP53	chr2	74691678	74691700	74691867	74691889	CTCTTGACGAACTGGTGGTGAGCCTTAAGGCCCC	CTCTTGACGAACTCAGTGGTGAGCCTTAAGGCCCC	MOGS-01
BSRI_HV_AMP54	chr2	136872764	136872787	136872982	136873003	ATGAGGATGACTGTTGAGGGCCTTGGGCTCACA4	ATGAGGATGACTGTTGAGGGCCTTGGGCTCACA4	
BSRI_HV_AMP55	chr2	136873185	136873206	136873368	136873393	CAAAGTACCAGTTTCAATAAAATCTTCCTGCCCACC	CAAAGTACCAGTTTCGCACGGCATCAACTGCCCAG	CKCR4
BSRI_HV_AMP56	chr2	237998576	237998597	237998776	237998801	TACAACCATCATGAAGAAGCATGATTAGGGGCAAATC	TACAACCATCAAGCTGACCAGTGGTCTGAGCGCCOPS8-01;COPS8-02	
BSRI_HV_AMP57	chr2	238002713	238002735	238002924	238002949	ACCACCACCTCGCACTCCAAGAGATATTCTGTTCC	ACCACCACCTCCCACATGACAACAAGGAGACCOPS8-03	
BSRI_HV_AMP58	chr3	46415146	46415170	46415361	46415383	CAACATTGCCCTCTGCTGGAAAATAGAACAAC	CAACATTGCCCTCCAGGAATTCCR5	
BSRI_HV_AMP59	chr3	127778890	127778914	127779111	127779135	TCTTTTGTTCTGTGTAGTGACCCACTTGGAAAACA	TCTTTTGTTCTGTGTAGTGACCCACTTGGAAAACA	SEC61A1-02
BSRI_HV_AMP60	chr3	127779409	127779431	127779603	127779631	GCCTTGGCCTCCAGAAGAGATAAACCTAAAACTGAGAT	GCCTTGGCCTCGGTATTTCTCTCTTCATTGCAACTA	SEC61A1-03
BSRI_HV_AMP61	chr3	127785843	127785887	127786042	127786068	AGTACAACAGCTCATGAGCAAGACACTCTATCCTGT	AGTACAACAGCTATATCCCATCAAGCTCTTCTATAGGT	SEC61A1-01
BSRI_HV_AMP62	chr4	73957688	73957714	73957904	73957930	GGATATGCTA GAAGAATGGTTTGAAAAGCTCCTCAG	GGATATGCTAATGGAAGAGAAACTGGAAAACCAN	ANKRD17-01
BSRI_HV_AMP63	chr4	74000740	74000767	74000966	74000988	GCAGTCTTTTCATCAACAGCAGTGGTGGAAGAGC	GCAGTCTTTTCATGGTTTAAATTCTTCGAAGTTAAT	ANKRD17-03;ANKRD17-02
BSRI_HV_AMP64	chr4	83970944	83970973	83971129	83971162	GAATTGCCATTTAGAATAACTTTCCTATTTATTTT	GAATTGCCATTTAGCATTTTTCCDPS4-01;CDPS4-02	
BSRI_HV_AMP65	chr4	87968467	87968491	87968683	87968708	CCATGATAAAACATTTGGCAGGGCACTTTCAAGTC	CCATGATAAAGAGACCCCTCAAGACAGTTTGGTGHAFF1-02;AFF1-01	
BSRI_HV_AMP66	chr4	88055741	88055767	88055936	88055963	GTCACCATCCAGAAATATGCACTCTTCCTTTTCTC	GTCACCATCCAGAAATATGCACTCTTCCTATGTCACCAFF1-03	
BSRI_HV_AMP67	chr4	177241149	177241167	177241361	177241382	GATGCGAGGGGATGCCTCACTCACAGCATTGATC	GATGCGAGGGGCATGCCGCCGCCGGAACGGGCSPC3-01;SPC3-03	
BSRI_HV_AMP68	chr4	177249261	177249288	177249447	177249477	AAGTATTTGACATCTCAGTGTTTGTCTTAAAATTTSPC3-02	AAGTATTTGACATCTCAGTGTTTGTCTTAAAATTTSPC3-02	
BSRI_HV_AMP69	chr5	133311500	133311525	133311704	133311725	GGATTCCAACATAAAGAGCAGATGGGCCTGCCTG	GGATTCCAACATAAAGAGCAGATGGGCCTGCCTG	VDAC1-03
BSRI_HV_AMP70	chr5	133316477	133316497	133316729	133316751	GTCACTCGGGCACCCCACTCCCTTTATTTGAC	GTCACTCGGGCATGCCCCACTCCCTTTATTTGAC	VDAC1-01;VDAC1-02
BSRI_HV_AMP71	chr5	138651324	138651348	138651518	138651548	ACAAGGCTGTTTTGTGAAAAGGACAGTTTTATTTT	ACAAGGCTGTTTTGTGAAAAGGACAGTTTTATTTT	MATR3-03
BSRI_HV_AMP72	chr5	138652651	138652673	138652871	138652896	TTGTGTTTGGTCCCATAAGGACCAGGATACATAC	TTGTGTTTGGAAGATGCACGTTTTTCTAGTAAATT	MATR3-02
BSRI_HV_AMP73	chr5	138654431	138654461	138654658	138654684	GCCTCTTTTGTTTTGTATTTTTATCTGAAGATTAT	GCCTCTTTTGTTTTGTAAAGTATTTTATCTGAAGTAT	MATR3-01
BSRI_HV_AMP74	chr5	177019268	177019288	177019460	177019480	TGGGTAGAGTATCTCTAGAGAGGCTGACTGTCTCGC	TGGGTAGAGTGATGCGGACCCTCCTGCTGGTGCTMED9-03	
BSRI_HV_AMP75	chr5	177020608	177020634	177020809	177020840	ATCCCTACCATAATACTGACTGAAGCTTGTTACTT	ATCCCTACCATAATACTGACTGAAGCTGTTACTMED9-02	
BSRI_HV_AMP76	chr5	177020999	177021022	177021202	177021224	CATGCGGCTCAAGACACTCACTCAAAGAGGGCCAG	CATGCGGCTCAAGACACTCACTCAAAGAGGGCCAGTCTMED9-01	
BSRI_HV_AMP77	chr6	27839710	27839731	27839979	27839979	CGCAAGCTGGATGTCTTTAGGCATAATAGTGACTTH3I3-02;HST1H3I-01;HST1H3I-03	CGCAAGCTGGATGTCTTTAGGCATAATAGTGACTTH3I3-02;HST1H3I-01;HST1H3I-03	
BSRI_HV_AMP78	chr6	43492500	43492522	43492712	43492733	CCCAAGAGACTAGGAGCAGACGAGTGATGAAGXPO5-01	CCCAAGAGACTAGGAGCAGACGAGTGATGAAGXPO5-01	
BSRI_HV_AMP79	chr6	43498310	43498338	43498505	43498529	ATAATCTCATCCTTCCTTCCAGTTCTGCCTCTTCCCC	ATAATCTCATCCTTCCTTCCAGTTCTGCCTCTTCCCC	XPO5-02
BSRI_HV_AMP80	chr6	43516067	43516092	43516267	43516294	CGCTCGTAGTTGTTCAATTGGTTTCTTCTTTCTTCC	CGCTCGTAGTTGTTCAATTGGTTGCATATGAAGAACXPO5-03	
BSRI_HV_AMP81	chr8	74858803	74858836	74859045	74859075	ATAATTCTTTTCAACTGAACTACAGGTATTAAATACTGAAAAGCTCAATGGAACTACAGGTATTAAATACTGAAAAGCTCATCB1-03		
BSRI_HV_AMP82	chr8	74867987	74868014	74868173	74868199	GAGACTCTGTCAAAGAGAACATGCATTAACATCAGCGC	GAGACTCTGTCTCTCAAAACAAAAGAACAAAACTCB1-01	
BSRI_HV_AMP83	chr8	74868200	74868227	74868436	74868459	TTACAATAAATTATTAACAGACGGCTTGTTTGA	TTACAATAAATTATTAACAGACGGCATAGATATCAATCB1-02	
BSRI_HV_AMP84	chr8	109241229	109241255	109241411	109241438	TTTTCCTCATCGAATTGTTAAACAGGTTCCAGCAACAG	TTTTCCTCATCGAAAGTGTGAAGGATACACAGATEIF3E-01	
BSRI_HV_AMP85	chr8	109247209	109247237	109247382	109247412	ACATGTACTTATACCTCAAAGACTTATGAATTACAATGGG	ACATGTACTTATACTTACCAGCACTCTAAAAAAATTEIF3E-02	
BSRI_HV_AMP86	chr8	109254025	109254055	109254271	109254298	TACCATGAGAGTTGTTGTCATGTCATGAAATAAAGGTTTTTEIF3E-03	TACCATGAGAGTTGTTGTCATGTCATGAAATAAAGGTTTTTEIF3E-03	
BSRI_HV_AMP87	chr8	117658639	117658664	117658832	117658859	AAATTTCTCACTGTCTTCTGCTTCAGAAACGAATGAAT	AAATTTCTCACTGTCTTCTGCTTCTCAGAAACGAATEIF3H-03	
BSRI_HV_AMP88	chr8	117671039	117671066	117671222	117671249	ACCTCCTACTAACCATAAATGAGAAGCACAGATTCEIF3H-02;EIF3H-01	ACCTCCTACTAACCATAAATGAGAAGCACAGATTCEIF3H-02;EIF3H-01	
BSRI_HV_AMP89	chr9	15479531	15479559	15479727	15479754	AAATGGACTGTTTTGCCATCGAATTAAACTTTGAGTGC	AAATGGACTGTTTTGCCATCGAATCAAACAGCPS8P1-01	
BSRI_HV_AMP90	chr9	15506544	15506568	15506769	15506793	GCTAACAGGATCTACGTCTCATGAGTTCCAAAATTCC	GCTAACAGGACTTACGTCTCATGAGTTCCAAAATTCC	PSP1-02
BSRI_HV_AMP91	chr9	15510107	15510127	15510352	15510371	TCACTTACTCGGCCTTCGGGGTTCTTCGCCTT	TCACTTACTCGGACTGGCGAATGGGGATAACCTTTCEDGF;PSP1-03	
BSRI_HV_AMP92	chr9	102778583	102778606	102778854	102778854	TGGACAGTAGAAATAAGAATATAGCTTTTTGCAGCACAGG	TGGACAGTAGAAATAAGAATATAGCTTCCATTTTCAAFBP44-02	
BSRI_HV_AMP93	chr9	102784339	102784364	102784556	102784579	TTCTGCTAAGTCCCGAATTTCTTGAATGGGGTGACERP44-01;ERP44-03	TTCTGCTAAGTCCCGAATTTCTTGAATGGGGTGACERP44-01;ERP44-03	
BSRI_HV_AMP94	chr10	70097555	70097580	70097761	70097787	GGAATGTTTCGAACTTTAACACCATCCCAAACTCTCC	GGAATGTTTGAGCCTTTAACATCGTTCCCCTTGATHNRNPH3-03;HNRNPH3-02;HNRNPH3-01	
BSRI_HV_AMP95	chr10	72610832	72610855	72610957	72611081	TGGTTGCTATATCGAGGTGATAGAGACAAAATCACCCC	TGGTTGCTATATCGAGGTGATATCGTAGGAAATSGP1-02	
BSRI_HV_AMP96	chr10	72628022	72628045	72628219	72628243	CAAACATTGTCTGTACTCCAGACAGACAAATCCAA	CAAACATTGTGAAGATCAGGGCGATGAAGAGCCGCSGP1-01	
BSRI_HV_AMP97	chr10	72633121	72633146	72633341	72633364	CAAAAGGCTCCCAGTCTTCCACACATACTCTGA	CAAAAGGCTCATCATTGGTGTTGTATAGTGACAASGP1-03	
BSRI_HV_AMP98	chr11	14535095	14535118	14535264	14535294	AAAAGCAAGGCTGTCACTTACACTCCATAAATTCA	AAAAGCAAGGCTGTCACTTACACTCCATAAATTCA	PSMA1-03
BSRI_HV_AMP99	chr11	14539094	14539123	14539284	14539314	AGACAACTTCCACTTTATAATGTCTCTATTTAGAGGGCGC	AGACAACTTCCACAAATACCTTATCTGGATCTTTTTPSMA1-02;PSMA1-01	
BSRI_HV_AMP100	chr11	32610512	32610536	32610694	32610726	TGGTTGCTGATTCAAACATTGTTTATTTGTTTGTTEIF3M-03	TGGTTGCTGATTTCAAACATTGTTTATTTGTTTGTTEIF3M-03	
BSRI_HV_AMP101	chr11	32615307	32615332	32615519	32615541	GTCACGGTTATAATGTCATCAGCACAGTACCTGCCTEIF3M-02;EIF3M-01	GTCACGGTTATAATGTCATCAGCACAGTACCTGCCTEIF3M-02;EIF3M-01	
BSRI_HV_AMP102	chr11	118920203	118920224	118920429	118920450	CTCTCGCGCCTACTACCTCATCCCCCACCGTCTCCTGHPU31-01	CTCTCGCGCCTACTACCTCATCCCCCACCGTCTCCTGHPU31-01	
BSRI_HV_AMP103	chr11	118922265	118922289	118922489	118922510	AGAAGAGTACCCGTTTATTGTGCTTCAGGCTGTGCHPU31-03	AGAAGAGTACCCGTTTATTGTGCTTCAGGCTGTGCHPU31-03	
BSRI_HV_AMP104	chr11	118926775	118926797	118926998	118927021	TACATACCACACT GAGAAGGGAGAAGTAGGCTGATC	TACATACCACACTGGCCAAGGCAGGTCTGCCAAGAGHPU31-02	
BSRI_HV_AMP105	chr11	134046088	134046116	134046301	134046324	CGAAAGCTCAACAAATCCTACTTAACTCTAAACCAANCAP03-02	CGAAAGCTCAACAAATCCTACTTAACTCTAAACCAANCAP03-02	
BSRI_HV_AMP106	chr11	134047247	134047268	134047465	134047489	ATGATGAGGTTGTTGCGGAGAGCCAGTGCTCAGCNCAP03-03	ATGATGAGGTTGTTGCGGAGAGCCAGTGCTCAGCNCAP03-03	
BSRI_HV_AMP107	chr11	134093689	134093707	134093911	134093932	TTAGGCATCGTGGCCAGTGGGAGTAGTCTGTACG	TTAGGCATCGTGGGGAGGCGATAGGACCCTCGCCNCAP03-01	
BSRI_HV_AMP108	chr12	6925297	6925318	6925522	6925546	CAGTTGAAAAGCTGACGGGCGAGTGGCGAGCTGTCCDA-01	CAGTTGAAAAGCTGACGGGCGAGTGGCGAGCTGTCCDA-01	
BSRI_HV_AMP109	chr12	6926373	6926395	6926599	6926622	GAGAACAAGCCAGAGGGACACCATACCCATAACC	GAGAACAAGAGGCAAAGGTCTCGAAGCGGGACCDA-02	
BSRI_HV_AMP110	chr12	6928392	6928413	6928605	6928628	CCAATTGGAGG CAATGGCAAATTGTAGAGGAGGC	CCAATTGGAGGTGCTAGAACGCAAAGGGGTTGCACDA-03	
BSRI_HV_AMP111	chr12	7078542	7078564	7078748	7078772	AGCTCTTGCAGATGTGGAAAGAGGCCTAAAGGGTPHB2-03;PHB2-01	AGCTCTTGCAGATGTGGAAAGAGGCCTAAAGGGTPHB2-03;PHB2-01	
BSRI_HV_AMP112	chr12	7079476	7079497	7079704	7079724	CGCTGCTCAGAGGAAATGCTAGGCCCGTGGAGGTPHB2-02	CGCTGCTCAGAGGAAATGCTAGGCCCGTGGAGGTPHB2-02	
BSRI_HV_AMP113	chr12	16035647	16035667	16035898	16035921	AATGGAGACAGCCCGCTCAACCACTCCTTTCTCCAC	AATGAGACAGACGCCGCTCACCTCGCCTGGCCACASTRAP-01;STRAP-03	
BSRI_HV_AMP114	chr12	16048160	16048186	16048409	16048434	TTGTGACTTGGAATACTGGAATGTTTTTCTGTAATTSTRAP-02	TTGTGACTTGGAATACTGGATTTTTCTGTAATTSTRAP-02	
BSRI_HV_AMP115	chr12	49099454	49099481	49099671	49099697	GCATTGAAATACATAAAGATCCAGGCATGCTTGGCCNT1-03;CCNT1-02	GCATTGAAATACATAAAGATCCAGGCATGCTTGGCCNT1-03;CCNT1-02	
BSRI_HV_AMP116	chr12	49110352	49110376	49110552	49110573	GAAAGTTCTTTATCTGGGTCCGCGCAAAACGCAGCCCNT1-01	GAAAGTTCTTTATCTGGGTCCGCGCAAAACGCAGCCCNT1-01	
BSRI_HV_AMP117	chr13	25027674	25027697	25027873	25027896	AAAGCATGGTAGGAAAAGACCCAGGGAGATACAGCPARP4-01	AAAGCATGGTAGGAAAAGACCCAGGGAGATACAGCPARP4-01	
BSRI_HV_AMP118	chr13	25052349	25052371	25052595	25052622	ACGTCACAAGAAGCAGGAGGACTCTCGTGCCATCTGCPARP4-02	ACGTCACAAGAAGCAGGAGGACTCTCGTGCCATCTGCPARP4-02	
BSRI_HV_AMP119	chr13	25075721	25075746	25075931	25075959	GTGTACTATGTCTTAGATAATGCTGATGTTCTGAGTCA	GTGTACTATGCGACCTATGATACGTTAAATGCTTGPARP4-03	
BSRI_HV_AMP120	chr14	78174373	78174396	78174560	78174585	GAAGCAGATTCTCTCGTGTTCCGGATCGGAAATTSLIRP-01;SLIRP-02	GAAGCAGATTCTCTCGTGTTCCGGATCGGAAATTSLIRP-01;SLIRP-02	
BSRI_HV_AMP121	chr14	78183756	78183784	78183983	78184005	CTGACTCCCTAAGTTTGCAGTTTTGCAGTTTGAATGSLIRP-03	CTGACTCCCTAAGTTTGCAGTTTTGCAGTTTGAATGSLIRP-03	
BSRI_HV_AMP122	chr15	41535856	41535882	41536063	41536088	GCTCTTTAGTTTCCCACAGTCAACTCATCGCCTCTCHP1-01	GCTCTTTAGTTTCCCACAGTCAACTCATCGCCTCTCHP1-01	
BSRI_HV_AMP123	chr15	41554913	41554938	41555085	41555113	GTGATTGACATGGTGTTTGTGTTTGTTATATTTCACHP1-02	GTGATTGACATGGTGTTTGTGTTTGTTATATTTCACHP1-02	
BSRI_HV_AMP124	chr15	41562742	41562767	41562964	41562990	TTTTCCCTTACAGCTTACCTTTTCGACTATATGATTTGCHP1-03	TTTTCCCTTACAGCTTACCTTTTCGACTATATGATTTGCHP1-03	
BSRI_HV_AMP125	chr16	2825337	2825358	2825561	2825583	CGAGGAAGACTGCCCTGAAGGCTTCAAGCCTTCACTCCA	CGAGGAAGACACTGCCCTGAAGGCTTCAACTCCATCB2-03	
BSRI_HV_AMP126	chr16	2826903	2826924	2827108	2827129	GCCGCTACTGTTTACATCGCGGACAGGGTAGGCGCTCB2-01;TCEB2-02	GCCGCTACTGTTTACATCGCGGACAGGGTAGGCGCTCB2-01;TCEB2-02	
BSRI_HV_AMP127	chr16	30506107	30506128	30506310	30506332	TTGGTGCCGCCGTTCTATAGGGGAGCAGAGAGAGTCGAC	TTGGTGCCGCCGTTCTATAGGGGAGCAGAGAGAGTCGAC	
BSRI_HV_AMP128	chr16	30507646	30507667	30507873	30507895	ATTCTCAGGTCCATCTCACCTCAGCACGGATCAT	ATTCTCAGGTGCCCTAAGCCCCAAGCCCAGACCGTGAL-01	
BSRI_HV_AMP129	chr16	30529028	30529049	30529222	30529244	TATGGGGCGTGCTGCACATCTCTTAGGAGCGGGG	TATGGGGCGTGGAGCTGAGAGACGGTGGGGCCTGTGAL-02	
BSRI_HV_AMP130	chr16	67063534	67063554	67063710	67063730	GCCGCCTGCTTGCCGCAGCGGACTCATTTTTC	GCCGCCTGCTTGCCGCCTTATCGGCGGCTGGGACTCBFB-01;CBFB-03	
BSRI_HV_AMP131	chr16	67132525	67132551	67132720	67132747	CTGTGTGCTACTGTCTTGTATTTTGTATATCTAGTTCBFB-02	CTGTGTGCTACTGTCTTGTATTTTGTATATCTAGTTCBFB-02	
BSRI_HV_AMP132	chr16	74334906	74334934	74335129	74335155	GTTTCT

Supplementary Figure 1

A.

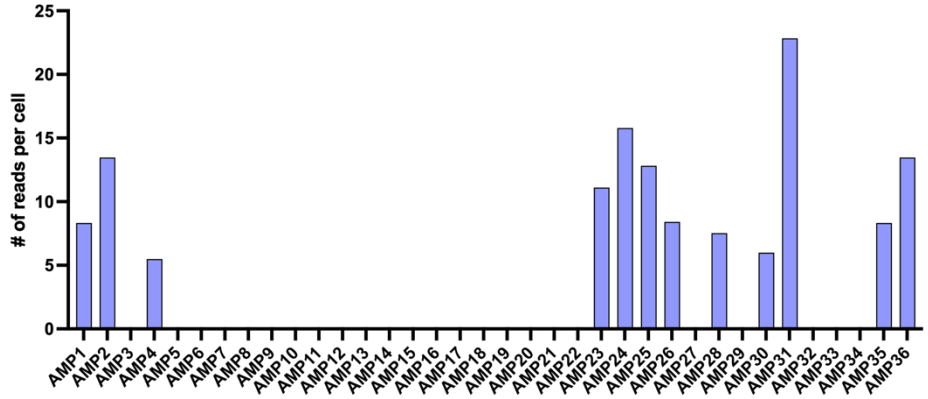

B.

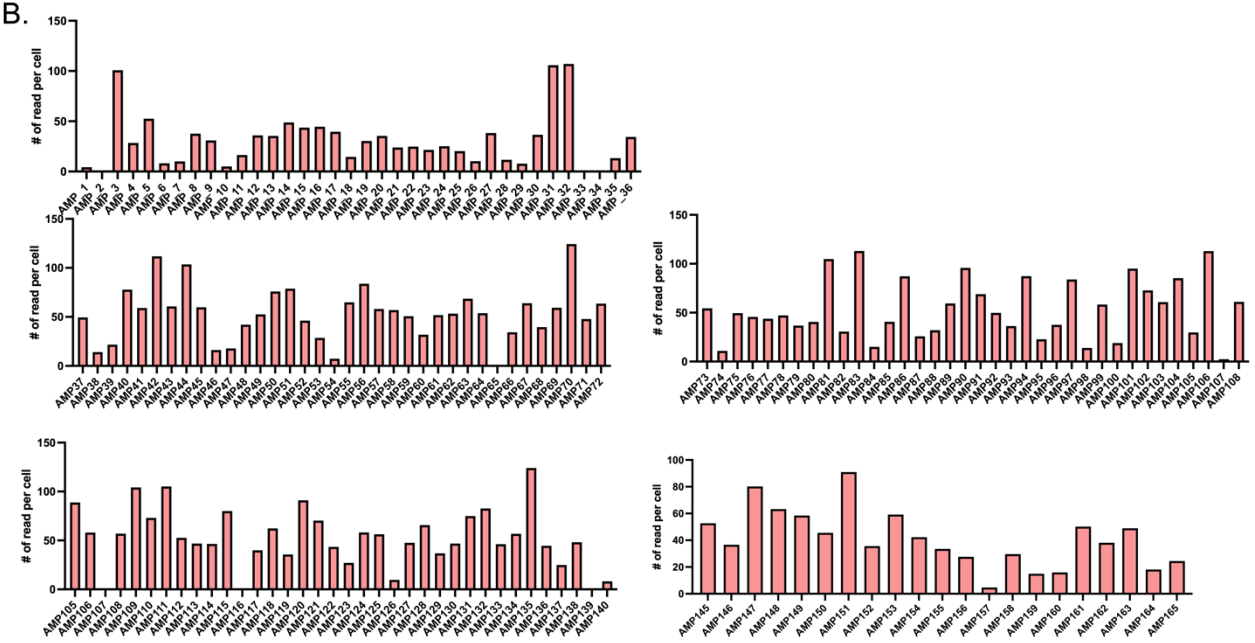

C.

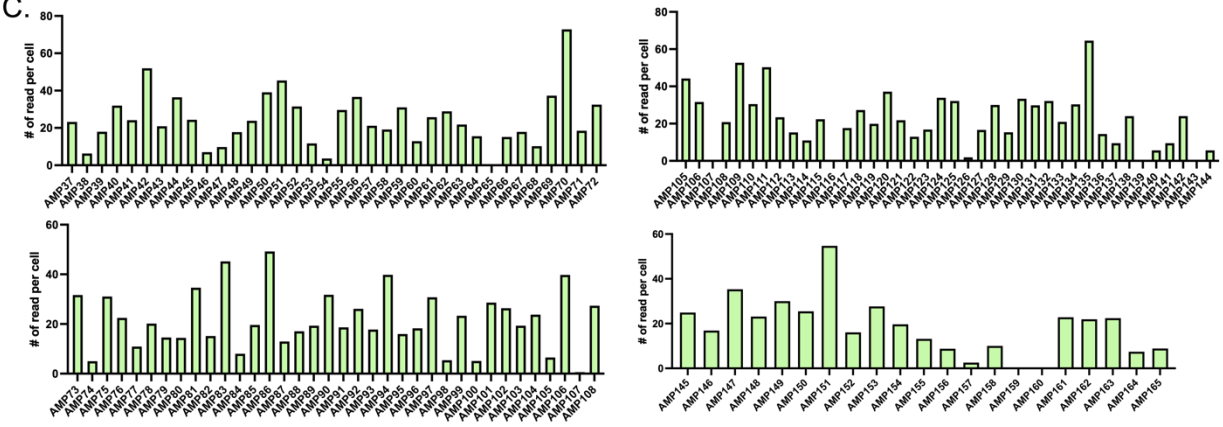

Supplementary Figure 2

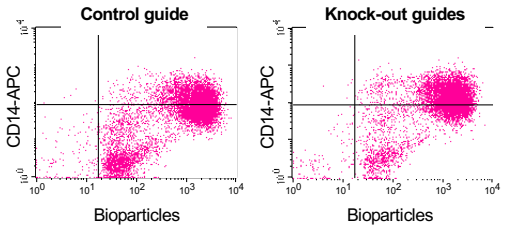

Sample	Phagocytic Index (%)	Green MFI in CD14+ Bioparticle+
Control guide	99.86	1756.6
Knock-out guides	99.90	1595.8